

2

Urban Climate Science

Coordinating Lead Authors

Daniel A. Bader (New York), Reginald Blake (New York/Kingston), Alice Grimm (Curitiba)

Lead Authors

Rafiq Hamdi (Brussels/Oujda), Yeonjoo Kim (Seoul), Radley Horton (New York), Cynthia Rosenzweig (New York)

Contributing Authors

Keith Alverson (Nairobi), Stuart Gaffin (New York), Stuart Crane (Nairobi/London)

This chapter should be cited as

Bader, D. A., Blake, R., Grimm, A., Hamdi, R., Kim, Y., Horton, R., and Rosenzweig, C. (2018). Urban climate science. In Rosenzweig, C., W. Solecki, P. Romero-Lankao, S. Mehrotra, S. Dhakal, and S. Ali Ibrahim (eds.), *Climate Change and Cities: Second Assessment Report of the Urban Climate Change Research Network*. Cambridge University Press. New York. 27–60

What Cities Can Expect

People and communities around the globe are reporting weather events and patterns that seem unfamiliar. Such changes will continue to unfold over the coming decades and, depending on which choices people make, possibly for centuries. But the various changes will not occur at the same rates in all cities of the world, nor will they all occur gradually or at consistent rates of change.

Climate scientists have concluded that, whereas some of these changes will take place over many decades, even centuries, there is also a risk of crossing thresholds in the climate system that cause some rapid, irreversible changes to occur. One example would be melting of the Greenland and West Antarctic ice sheets, which would lead to very high and potentially rapid rates of sea level rise in many cities.

Major Findings

- Urbanization tends to be associated with elevated surface and air temperature, a condition referred to as the *urban heat island (UHI)*. Urban centers and cities are often several degrees warmer than surrounding areas due to presence of heat-absorbing materials, reduced evaporative cooling caused by lack of vegetation, and production of waste heat.
- Mean annual temperatures in 153 ARC3.2 cities around the world are projected to increase by 0.7 to 1.6°C by the 2020s, 1.4 to 3.1°C by the 2050s, and 1.7 to 5.0°C by the 2080s. Mean annual precipitation in 153 ARC3.2 cities around the world is projected to change by –7 to +10% by the 2020s, –9 to +14% by the 2050s, and –11 to +20% by the 2080s. Sea level in 71 ARC3.2 coastal cities is projected to rise 4 to 18 cm by the 2020s; 14 to 56 cm by the 2050s, and 22 to 118 cm by the 2080s (see Annex 2, Climate Projections for ARC3.2 Cities).
- Some climate extremes will be exacerbated under changing climate conditions. Extreme events in many cities including

heat waves, droughts, heavy downpours, and coastal flooding are projected to increase in frequency and intensity.

- The warming climate combined with the UHI effect will exacerbate air pollution in cities.
- Cities around the world have always been affected by major, naturally occurring variations in climate conditions including the El Niño Southern Oscillation, North Atlantic Oscillation, and the Pacific Decadal Oscillation. These oscillations occur over years or decades. How climate change will influence these recurring patterns in the future is not fully understood.

Key Messages

Human-caused climate change presents significant risks to cities beyond the familiar risks caused by natural variations in climate and seasonal weather patterns. Both types of risk require sustained attention from city governments in order to improve urban resilience. One of the foundations for effective adaptation planning is to co-develop plans with stakeholders and scientists who can provide urban-scale information about climate risks – both current risks and projections of future changes in extreme events.

Weather and climate forecasts of daily, weekly, and seasonal patterns and extreme events are already widely used at international, national, and regional scales. These forecasts demonstrate the value of climate science information that is communicated clearly and in a timely way. Climate change projections perform the same functions on longer timescales. These efforts now need to be carried out on the city scale.

Within cities, neighborhoods experience different microclimates. Therefore, urban monitoring networks are needed to address these unique challenges and the range of impacts from extreme climate effects at neighborhood scales. The observations collected through such urban monitoring networks can be used as a key component of citywide climate indicators and monitoring systems that enable decision-makers to understand and plan for a variety of climate risks across the city urban landscape.

Note: Temperature and precipitation projections are based on 35 global climate models and 2 representative concentration pathways (RCP4.5 and RCP8.5). Timeslices are 30-year periods centered around the given decade (e.g., the 2050s is the period from 2040 to 2069). Projections are relative to the 1971 to 2000 base period. For each of the 153 cities, the low estimate (10th percentile) and high estimate (90th percentile) was calculated. The range of values presented is the average across all 153 cities. Sea level rise projections are based on a 4-component approach that includes both global and local factors. The model-based components are from 24 global climate models and 2 representative concentration pathways (RCP4.5 and RCP8.5). Timeslices are 10-year periods centered around the given decade (e.g., the 2080s is the period from 2080 to 2089). Projections are relative to the 2000 to 2004 base period. For each of the 71 cities, the low estimate (10th percentile) and high estimate (90th percentile) was calculated. The range of values presented is the average across all 71 coastal ARC3.2 cities. ARC3.2 Cities include Case Study Docking Station cities, UCCRN Regional Hub cities, UCCRN project cities, and cities of ARC3.2 Chapter Authors.

Like all future projections, UCCRN climate projections have uncertainty embedded within them. Sources of uncertainty include data and modeling constraints, the random nature of some parts of the climate system, and limited understanding of some physical processes. In the ARC3.2 Report, the levels of uncertainty are characterized using state-of-the-art climate models, multiple scenarios of future greenhouse gas concentrations, and recent peer-reviewed literature. The projections are not true probabilities, and scenario-planning methods should be used to manage the risks inherent in future climate.

2.1 Introduction

Urban areas have special interactions with the climate system that produce heat islands, reduce air quality, and exacerbate runoff. This chapter presents information about these processes, observed climate trends, extreme events, and climate change projections for cities. It is essential that this information be developed and communicated in ways that contribute to science-based decisions made by city managers to enhance climate resilience.

Section 2.2 introduces the co-generation process that can be used to develop urban climate risk information. Section 2.3 provides an overview of the urban climate system, including a discussion of the urban heat island (UHI), air quality, and the role of urban monitoring networks. Section 2.4 describes the role of natural variability in influencing urban climate risk and how lessons from communicating seasonal climate forecast information may translate to future climate change action. Section 2.5 discusses observed climate trends in cities and the influence that urbanization may be having on these trends. Section 2.6 focuses on how climate change is projected to impact cities in the future and how climate science information, including projections, is being used for adaptation and resilience planning.

Throughout the chapter, city examples and focused case studies are provided to emphasize the key themes of urban climate science, which include urban vulnerability to extreme climate events and the need to advance the science (including climate science) of urban adaptation assessment and implementation.

2.2 Co-generation of Urban Climate Risk Information

The information about urban climate processes, observed climate trends, extreme events, and climate change presented in this chapter is tailored to support the decisions that city stakeholders make in planning for climate resilience. The development of climate risk information for cities is an interactive and iterative process between scientists and stakeholders. To improve policy efforts for enhancing resilience in urban settings, city managers need to identify key stakeholders, engage scientists in the process of risk analysis, work with specialized experts in the co-generation of climate information, and maintain lines of communication among the various groups. A growing body of literature supports the need for adaptation planning grounded in climate science (Moss et al., 2013; Lemos et al., 2013; Kerr, 2011).

The potential for and current use of scientific information in urban decision-making demonstrates the importance of improved communications. The diversity of urban systems and

urban climate science topics makes dissemination of information outside of the scientific community a daunting task; standardization of terminology and classification of phenomena can help to improve the dialogue (Oke, 2006). The numerous different foci of urban climate science research are exemplary of its large scope, and illustrate the large scope for further research on the use of scientific information in urban planning.

The complexity of cities presents unique challenges and opportunities for knowledge co-generation. Given the wide range of systems, operations, and perspectives that are characteristic of cities, an array of stakeholder representation has become a necessary complement to the knowledge co-generation process. Developing climate information with multi-sector considerations requires the bringing together of governmental and non-governmental organizations (NGOs), “knowledge providers” with scientific backgrounds, business leaders, planners, and utilities experts. By utilizing a framework that includes global climate scenarios, the exchange of local climate change data, and the illustration of socioeconomic and climate risk factors, such groups can communicate constructively and develop salient and usable local data. The use of remote sensing tools and the establishment of urban monitoring networks can enhance understanding of urban climate effects, helping to ensure that adaptation planning is grounded in science. Regular and iterative interactions among these stakeholder groups and scientists can produce climate risk information that is vital to a city’s resilience planning and implementation (New York City Panel on Climate Change [NPCC], 2015) (see Figure 2.1).

Local climate risk information is an essential component of a city’s comprehensive framework for responding to the risks of climate variability and change and to its implementation of adaptation strategies. This underlying climate science is critical for identifying vulnerabilities and for planning a response for urban resilience that integrates and is predicated on the ongoing development of scientific knowledge. Interactions between scientists and stakeholders, taking into consideration the many components of the urban climate system, lead to the co-generation of usable information that aids in the understanding of climate risk and in the planning for resilient cities. It is this collaboration between the climate science providers and the decision-makers that generates useful and practical climate science information that is needed to address the challenges that arise when climate change adaptation initiatives are implemented in urban areas.

2.3 Urban Climate Processes

A thorough understanding of the urban climate system is the starting point for the climate risk assessment process. Critical to this is the need for long-term, quality-controlled, observed climate data. In many cities, especially those in developing countries, the historical record is short and/or discontinuous or of uncertain quality. This makes trend analysis and climate change detection difficult. Without long-term historical records,



Figure 2.1 Wetland restoration in New York, where co-generated climate science information is guiding the city's resiliency efforts.

Source: New York City Department of City Planning

the role of climate variability cannot be adequately described, and climate change projections will not be supported by a strong historical baseline (Blake et al., 2011 and references therein). Even in places where a long-term record is available, there often exists scope to expand urban climate monitoring networks to better understand within-city variations and improve awareness of climate risks.

Understanding how the urban climate (e.g., temperature, precipitation, and winds) varies within cities has important implications for stakeholders when developing adaptation strategies. With a greater understanding of the microclimate environment, recognition of key vulnerabilities can advance, leading to targeted adaptation responses. All of the urban effects described here can impact city systems with varying magnitudes depending on the relative importance of climate hazards for a particular location.

This section describes the key components of the urban climate system and urban climate monitoring networks.

2.3.1 Urban Heat Island

Urbanization is often associated with elevated surface and air temperature, a condition referred to as the *urban heat island* (see Case Study 2.1 and Box 2.1). Urban centers and cities are often several degrees warmer than their surrounding areas (see Table 2.1). Due to the low albedo (reflectivity) of urban surfaces such as rooftops and asphalt roadways, the trapping of radiation within the urban canopy, differential heat storage, and greater surface roughness, cities “trap” heat (Oke, 1978). The reduction in evapotranspiration due to impervious surfaces also contributes to the UHI. In addition, the high density of urban environments often leads to intense anthropogenic heat releases within small

spatial scales – particularly from critical urban infrastructure systems such as transportation and energy – that can enhance the UHI by up to 1°C (Ohashi et al., 2007; Tremeac et al., 2012; Zhang et al., 2013a).

Urban sectors, such as energy and health, are readily influenced by the UHI effect. A study of a small city in western Greece found greater (lower) cooling (heating) demands in the summer (winter) in the urban center as compared to surrounding rural locations (Vardoulakis et al., 2013). A study of the heat island in Shanghai, China, found heightened heat-related mortality in urban regions, with worsening health effects from higher temperatures (Tan et al., 2010). The combined effects of increasing heat waves due to climate change and the UHI effect also pose serious health risks to urban populations (Li and Bou-Zeid, 2013).

In one study, three factors contributing to the UHI (urban geometry, impervious surfaces, and anthropogenic heat releases) were analyzed for their relative importance and combined effects. Results showed that, during the day, heat island intensity tends to be driven by impervious surfaces, whereas in the evening anthropogenic heat is the main factor (Ryu and Baik, 2012). Regional climate models (see Section 2.6) can be used to investigate the importance of these factors and their effect on heat islands (Giannaros et al., 2013; Chen et al., 2014). In addition, regional climate models also are used to understand how physical processes in the background climate and geography also contribute to UHI (Zhao et al., 2014).

A large body of research on the mechanisms of the UHI is focused on land use, land surface characteristics, and surface temperatures. An analysis of the heat island in Rotterdam found that the heat island is largest for parts of the city with limited

Box 2.1 NASA Monitoring of Urban Heat Islands

The National Aeronautics and Space Administration (NASA) missions and instruments play a critical role in the monitoring of urban microclimates, including the urban heat island (UHI) effect. Satellite remote sensing instruments (such as the Moderate Resolution Imaging Spectroradiometer [MODIS] and the Landsat satellite) are important tools used by researchers in cities around the globe to investigate how urbanization influences surface–air heat fluxes and how UHIs evolve with time. Images captured from the instruments help to identify the magnitude and spatial scale of microclimates, as well as to infer land surface types and changes that also impact the urban environment.

Using MODIS data, a study of the heat island in Milan identified two different heat island phenomena present in the city, one throughout the day (the surface UHI) and one present only during the evening (the canopy layer heat island) (Anniballe et al., 2014). In another study, Landsat thermal images were used to calculate the intensity and spatial extent of the heat island in Brno, Czech Republic (Dobrovlny, 2013). A study of



Box 2.1 Figure 1 Urban heat island in Buffalo, New York measured by NASA satellites. Bright colors indicate higher temperatures, which are associated with more urbanized areas.

Source: NASA

Bucharest (Cheval and Dumitrescu, 2009) used MODIS data to study the spatial extent and the intensity of the heat island of that city.

Analyses across multiple cities in North America (Imhoff et al., 2010) and Asia (Tran et al., 2006) are further examples of how NASA instruments are being utilized to better understand urban microclimates. For all thirty-eight cities analyzed in Imhoff et al. (2009), impervious surface area (measured by Landsat) was identified as the primary driver of urban heating, which explains 70% of the total variance in land surface temperature (measured by MODIS). In Tran et al. (2006), data from both Landsat and MODIS were used to explore results between UHIs and land surface type in Bangkok and Ho Chi Minh City, with the research showing that both vegetation and urban density influenced microclimates in those cities.

The images and analysis that are produced from tools such as MODIS and Landsat can contribute to urban planning and the development of adaptation strategies. Imhoff et al. (2010) found that in North American cities in forested biomes, the summertime heat island tends to be much stronger than that in winter. This finding has implications for energy demand because increased urbanization could require additional cooling in these regions. The effectiveness of climate change adaptation and mitigation strategies, such as increasing green spaces, parks, and vegetated areas, can also be evaluated through NASA remote sensing products. Such analysis has already been completed for Chicago (Mackey et al., 2012) and Tel Aviv (Rotem-Mindali et al., 2015), with results indicating that greening techniques have the ability to reduce the impacts of the heat island.

In addition to enabling a better understanding of the urban environment, the data collected from remote sensing monitoring systems can supplement (or serve as an alternative to) observed station-based data and be used to develop standardized metrics for cross-city comparison of heat islands and other urban phenomena.

vegetation and large amounts of impervious surface (and thereby a low albedo; Klok et al., 2012). Similar results were found in a study of Toronto, Canada (Rinner and Hussain, 2011) and Phoenix, Arizona, with a study finding that changes in the configuration of grass and impervious surfaces explained temperatures in industrial and commercial areas, whereas the proportion of land cover of grass and impervious surfaces alone best explained temperatures in residential areas (Connors et al., 2013). Land use and land cover changes and population shifts also have influences on UHIs (Zhang et al., 2013b).

In some locations, such as New York, within-city temperature variations, which can be attributed to the UHI or other factors such as wind direction and proximity to water (Rosenzweig et al., 2009), can be as large as the projected changes between the late 20th and the late 21st centuries (e.g., Horton et al., 2011; Rosenzweig and Solecki, 2010). The UHI intensities in Tokyo, Shanghai, and Delhi (ranging from 3 to 12°C) already exceed the mean temperature increases projected for these cities by the 2080s (1.5–2.5°C)¹ (Blake et al., 2011) (see Table 2.1).

¹ For a description of the methods used for these climate projections, see Chapter 3 (Blake et al., 2011) of the *First UCCRN Assessment Report on Climate Change and Cities* (Rosenzweig et al., 2011).

Case Study 2.1 Urban Heat Island in Brussels

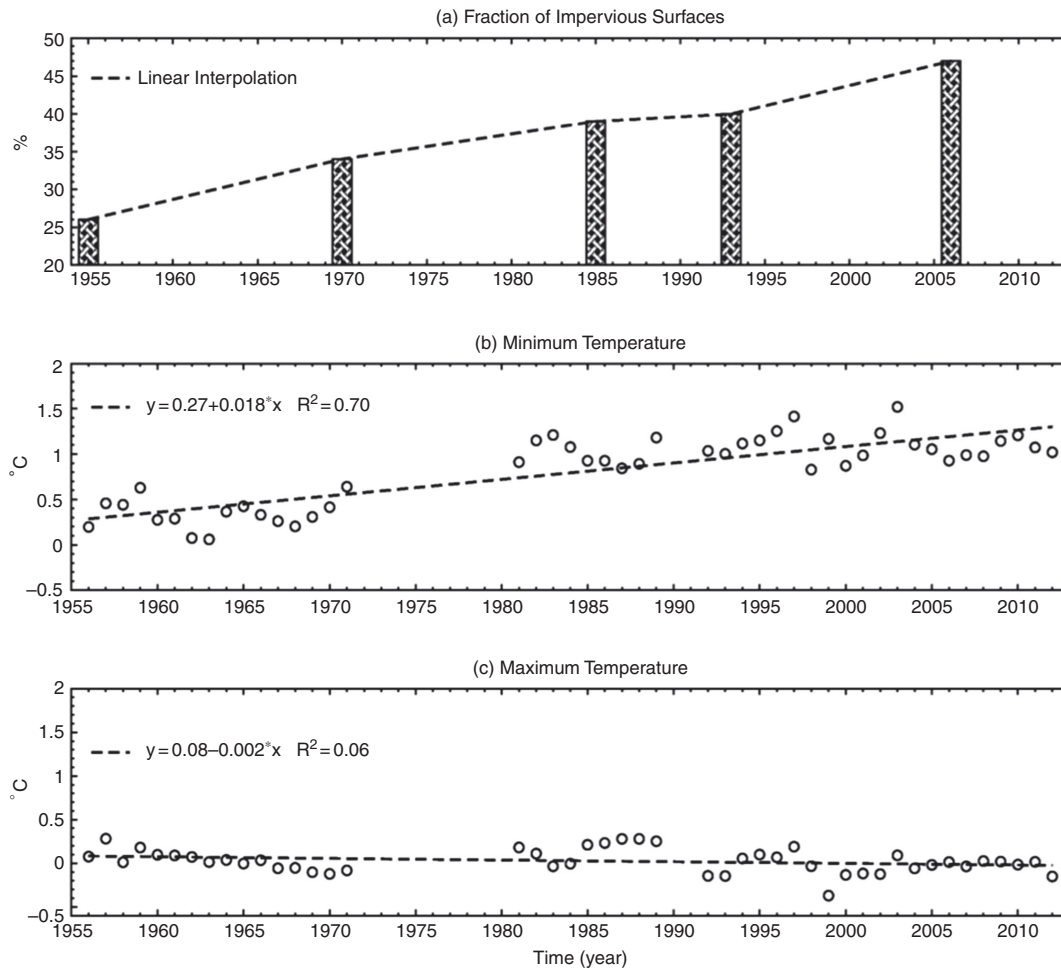
Rafiq Hamdi

Royal Meteorological Institute of Belgium, Brussels

Keywords	Urban heat island effect, urban growth, impervious surfaces, minimum temperature increase
Population (Metropolitan Region)	2,061,000 (UN, 2016)
Area (Metropolitan Region)	161.38 km ² (Brussels Statistics, 2015)
Income per capita	US\$46,010 (World Bank, 2017)
Climate zone	Cfb – Temperate, without dry season, warm summer (Peel et al., 2007)

The Brussels Capital Region (BCR) in Belgium has experienced a rapid transformation of agricultural land and natural vegetation to built areas (e.g., buildings, impermeable pavements) over the past century. There has been a rapid expansion of the city since the 1950s. The acceleration of urban growth is linked to widespread use of the car as a new mode of transport (Fricke and Wolf, 2002). The evolution of the fraction of impervious surfaces over the BCR since 1955 was studied by Vanhuysee et al. (2006). The results indicate a sharp increase in impervious surfaces areas, nearly a doubling from 26% in 1955 to 47% in 2006.

At the same time, a gradual increase in temperature has been observed at the national recording station of the Royal Meteorological Institute (RMI) of Belgium, located just south of the center of the capital in the Uccle suburb. This time series has a long history dating back to 1833 and has been homogenized within the EU IMPROVE project (Camuffo and Jones, 2002).²



Case Study 2.1 Figure 1 (a) Evolution of the average percent imperviousness of the Brussels Capital Region from 1955 to 2006; (b) and (c), annual mean urban heat island (UHI) effect on minimum and maximum, near-surface air temperature observed at Uccle, estimated as the difference with the rural climatological stations, with the linear trend, 1956–2012. R^2 is the coefficient of determination. The annual mean maximum temperature is substantially less affected by urbanization than the annual mean minimum temperature, which is consistent with previous studies in other cities (Landsberg, 1981; Kalnay and Cai, 2003; Hua et al., 2008). The increase of annual mean urban bias on minimum temperature may be attributed to: (1) higher thermal inertia, which, in combination with lower albedo of urban surfaces, delays the cooling of the cities at nights compared to rural areas (Hamdi and Schayes 2008) (2) limited evapotranspiration that prevents evaporative cooling of urban areas, and (3) the contribution of anthropogenic heat during night hours, which can also influence the long-term trend of near-surface air temperature.

It is important to understand whether, and to what extent, estimates of warming trends at Uccle can be explained by the growth of the UHI of the city of Brussels due to urban sprawl. If observations of near-surface air temperatures in growing cities are used in the assessment of global warming trends, these trends may be overestimated.

Two stations belonging to the RMI climatological network, situated 13 kilometers away from the center of Brussels are used to assess the degree to which the Uccle near-surface temperature trends are amplified by urbanization.³

The UHI intensity is defined as the difference in near-surface air temperature between urban and rural stations. Estimates of urban bias (influences of urbanization on the observed trend) at the Uccle recording station on annual-mean minimum and maximum temperature calculated between 1956 and 2012 are plotted with the linear trends in Case Study 2.1 Figure 1. The UHI effect on minimum temperature is shown to be rising with increased urbanization, with a linear trend of 0.18°C ($\pm 0.02^\circ\text{C}$) per decade. The coefficient of determination is $R^2 = 0.70$, which indicates a strong dependence between the increase of urban bias on minimum temperature and the changes in the percentage of impervious surfaces.

Table 2.1 Examples of cities with urban heat and urban precipitation islands

City	Effect observed	Urban Heat Island intensity ($^\circ\text{C}$)	Source	Urban Precipitation Island intensity (%)	Source
Athens	UHI	3.6	Kastoulis <i>et al.</i> , 1985	N/A	N/A
Cairo	UHI and UPI	1–4.5	Robaa, 2003	33–47	Robaa, 2003
Delhi	UHI	3.8–7.6	Mohan <i>et al.</i> , 2009	N/A	N/A
Houston	UHI and UPI	2–3	Streutker, 2003	22–25	Burian and Sheppard, 2005
Melbourne	UHI	–3.2–6	Morris <i>et al.</i> , 2000	N/A	N/A
Mexico City	UHI and UPI	3–7.8	Jauregui <i>et al.</i> , 1997	70	Jauregui, 1996
New York	UHI	1.5–8	Gaffin <i>et al.</i> , 2008 and Gedzelman <i>et al.</i> , 2003	N/A	N/A
São Paulo	UHI	5–10	Sobral, 2010	N/A	N/A
Shanghai	UHI and UPI	0.7–3	Jiong, 2004 and Hung <i>et al.</i> , 2006	5–9	Jiong, 2004
Tokyo	UHI	4–12	Hung <i>et al.</i> , 2006	N/A	N/A

2.3.2 Urban Precipitation, Moisture, and Wind Effects

Besides temperature, the dense urban environment can also have impacts on other climate variables (see Table 2.1). For example, there is evidence that precipitation can be enhanced downwind of highly urbanized areas (Burian and Shepherd, 2005; Shepherd, 2006; Han *et al.*, 2014). One possible mechanism for this is that the buildings within a city provide a source of lift for air, which, combined with a destabilized environment due to the heat island, leads to cloud development and precipitation (Shepherd *et al.*, 2010). Regional climate models (RCMs) (see Section 2.6) have been used to simulate precipitation patterns

near urban centers and investigate the extent to which urbanization influences them. A study analyzing precipitation in Tokyo, Japan, found that precipitation in the city is enhanced by urbanization, with the regional climate model able to simulate the effects (Hiroyuki *et al.*, 2013). RCM simulations of precipitation in the Baltimore-Washington metropolitan area show that urban surface characteristics, such as the presence of buildings, paved roads, and mass vehicle use, influence rainfall patterns (Li *et al.*, 2013; Li and Bou-Zeid, 2013). Although these studies have supported the hypothesis of urbanization influencing local precipitation, other studies (looking at cities in Turkey) found no evidence that urbanization affects local precipitation patterns (Tayanc and Toros, 1997).

² Corrections due to non-climatic factors such as changes in observation time, instrumentation, and relocation from the Gate of Schaerbeek in the city center to the Plateau of Uccle in 1890 were taken into account. More details about the homogenization of the time series of Uccle can be found in Demarée *et al.*, 2002.

³ Without assurance of homogeneity, trend estimates are unreliable, and artifacts in long-term observations and rural/urban differences can be introduced and may bias the estimate of the UHI. For this reason, the assumption that the three rural sub-series could be linked to constitute a reference rural series was tested with respect to data homogeneity (see Hamdi and Van De Vyver, 2011 for full information on the testing methods).

There are also examples of greater incidence of extreme precipitation events over cities – one study noted 35% more heavy downpours over Houston, Texas, compared to adjacent rural areas, possibly due to enhanced convection due to the UHI (Burian and Shepard, 2005). The urban environment may also influence thunderstorm composition and structure. A study of storm progression across Indianapolis, Indiana, found that more than 60% of storms change structure over the city itself, compared to only 25% when passing over surrounding rural regions (Niyogi et al., 2010). This effect was more likely during the daytime. This study also used regional climate models to verify the influence urban areas have on the thunderstorms, with simulations unable to model the thunderstorms without the inclusion of the urbanized Indianapolis region. Whereas these two examples reveal that urban areas may be enhancing convective precipitation, other studies suggest that increased aerosol concentrations in urban areas can “interrupt” precipitation formation processes and thereby reduce heavy rainfall (Seifert et al., 2012).

An additional urban phenomenon, urban moisture excess (e.g., Holmer and Eliason, 1999; Kuttler et al., 2007) or the *urban moisture island* (Richards, 2005) refers to conditions where higher humidity values are observed in cities relative to more rural locations. The primary mechanisms for these differences are evaporation, condensation, advection, and anthropogenic emissions of water vapor. Thessaloniki, Greece, is one city where observations show that the urban center is moisture-rich compared to its surrounding, semi-rural areas; this condition is more prevalent at nighttime (Giannaros and Melas, 2012).

Cities can also experience faster or slower wind speeds compared to their adjacent suburbs and countryside. Although urban structures increase the roughness of the land surface and present a widespread impediment to wind, periods of strong convection in the urban heat island can overcome the friction effect and cause locally elevated wind speeds (Lee, 1979). The net result is that the urban boundary layer tends to weaken

winds that are fast and strengthen winds that are slow (Childs and Raman, 2005). Street-scale studies have indicated that channeling is a prominent feature at the neighborhood level, increasing wind speeds in street canyons parallel to the prevailing winds and decreasing them in perpendicular ones (Dobre et al., 2005).

There is also evidence of interactions between the different microclimate effects. For example, in Melbourne, wind speed and cloud cover were linked to the strength of the UHI (Morris et al., 2001). Regional climate modeling of the UHI near Taipei, Taiwan, simulated how enhanced temperatures affect the location of precipitation and thunderstorms near the city (Lin et al., 2011). A study of streamflow near Ottawa, Canada, linked reduced severity of spring floods to the UHI effect (Adamowski and Prokoph, 2013). Placing these research results into the context of city decision-making, the findings from such studies could be of relevance to water managers in cities around the globe. The complexity and connections between the many urban climate effects reveals the need for continued advances in modeling and observational analysis.

2.3.3 Urban Climate Monitoring Networks

Using a network of weather monitoring stations and both satellite and ground-based remote sensing instruments, urban meteorology networks track multiple climate variables (e.g., temperature, precipitation, humidity, and wind speed) at high/fine spatial and temporal resolutions and can be used for a variety of applications, including urban micrometeorology research, and real-time tracking of extreme weather events (Muller et al., 2013a). Improvements and expansion of these systems can further the understanding of urban microclimates and improve high-resolution climate data availability in cities. Several cities across the globe have already established urban monitoring networks, including Helsinki (Wood et al., 2013), Hong Kong (Hung and Wo, 2012), and Tokyo (Takahashi et al., 2009) (see Table 2.2).

Table 2.2 Examples of urban monitoring networks. Source: Adapted from Muller, 2013a.

City	Monitoring network	Description of network	Source
Berlin	Berlin City Measurement Network	City-scale operational and research network	http://www.geo.fu-berlin.de/en/met/service/stadtmetnetz/index.html
Helsinki	The Helsinki Testbed	Open research network, advance knowledge of mesoscale meteorology	Dabberdt <i>et al.</i> , 2005; Koskinen et al., 2011; http://testbed.fmi.fi/
Hong Kong	Community Weather-Information Network (Co-WIN)	City-scale network to engage communities, promote education, and raise awareness of urban environmental issues, such as climate change, acid rain, and urban heat island	Hung and Wo, 2012; http://weather.ap.polyu.edu.hk/
London	London Air Quality Network (LAQN)	Mesoscale air quality monitoring with meteorological variables	http://www.londonair.org.uk/

Table 2.2 (continued)

City	Monitoring network	Description of network	Source
New York	NYC Mesonet	Integration of existing meteorological station data to provide real-time modeling	http://nycmetnet.ccny.cuny.edu/index.php
Taipei	Taipei Weather Inquiry-Based Learning Network (TWIN)	City-scale education/public information network	Chang <i>et al.</i> , 2010; http://www.aiclass.com.tw/products.aspx?BookNo=weather_01
Tokyo	Metropolitan Environmental Temperature and Rainfall Observation System (METROS)	City-scale temperature and precipitation observing system	Mikami <i>et al.</i> , 2003; Takahashi <i>et al.</i> , 2009
Washington D.C.	DCNet	City-scale network for forecasting dispersion of hazardous materials	Hicks <i>et al.</i> , 2012

Knowledge of urban microclimates has been advanced through the use and development of city-scale climate monitoring networks. For example, data from the meteorological network in Atlanta show that the UHI can trigger convective rainfall activity in the city (Bornstein and Lin, 2000). Observations from the weather network in Paris have been used to validate computer model simulations of the city's urban temperature and humidity microclimates (Lemonsu and Masson, 2002). Understanding urban islands and microclimates within cities and their metropolitan areas allows for better identification of climate vulnerabilities and risks, thereby enhancing the initial steps of the adaptation process (Major and O'Grady, 2010).

Climate data are often lacking in many cities. These records serve as important tools for analyzing past and current climate risks and can help form the basis of future climate projections. Depending on the methodologies used for developing future climate projections (see Section 2.6), future modeled changes may be applied to observed climate data. Observed records are also of great importance for historical climate model validation. Although historical climate analysis can provide a basis for future planning, it is important to note that it is necessary for adaptation strategies to prepare for climate hazards beyond those already experienced (Milly *et al.*, 2008).

Whereas increasing the number of meteorological stations is an important step for improving climate data in urban areas and advancing knowledge on urban climate science, there is also a need to harmonize collection practices, instrumentation, station location, and quality controls across cities to facilitate collaborative research and adaptation initiatives (Muller *et al.*, 2013b). Novel techniques to increase the number of observations and improve data quality include Light Detection and Ranging (LIDAR), scintillometers⁴, and low-cost sensors (Basara *et al.*, 2011; Wood *et al.*, 2013). There also may be

opportunities to crowdsource climate data through citizen science, social media, amateur weather stations and equipment, smart devices such as cell phones, and mobile platforms (e.g., sensors mounted on motor vehicles) (Overeem *et al.*, 2013; Muller *et al.*, 2015).

As meteorological stations and networks expand across cities, additional climate variables may be tracked and adaptation planning efforts can advance. With knowledge of the strategies that can be used to protect against a particular climate hazard, the implementation can now be targeted toward the most vulnerable communities. If particular neighborhoods are more prone to extreme heat events, based in part on observations from urban temperature monitoring stations (both maximum and minimum), cooling resources could be allocated there when heat waves are forecast. Urban precipitation monitoring networks can be used to identify portions of cities that are most at risk of flooding from intense precipitation events. Planning efforts to reduce urban flooding, such as the cleaning of storm drains in advance of heavy rainfall, could be concentrated in those vulnerable areas identified by the monitoring network (City of New York, 2013).

Data from meteorological networks in urban areas can also be used to evaluate the effectiveness of adaptation strategies. In Oberhausen, Germany, a network of meteorological observing stations was used to assess the potential of blue and green infrastructure to increase thermal comfort and reduce the thermal load of the city (Müller *et al.*, 2013; Goldbach and Kuttler, 2013).

Urban monitoring is also done for mitigation as well as for adaptation and resilience purposes. For example, the Los Angeles Megacities Carbon Project tracks carbon dioxide, methane, and carbon monoxide with surface and satellite instruments (see Case Study 2.2).

⁴ A scintillometer is a scientific device used to measure small fluctuations of the refractive index of air caused by variations in temperature, humidity, and pressure. These instruments can measure the transfer of heat between the Earth's surface and atmosphere. Such measurements can be used to better understand the UHI effect.

Case Study 2.2 Los Angeles Megacities Carbon Project

Riley Duren

NASA Jet Propulsion Laboratory, California Institute of Technology, Pasadena

Kevin Gurney

Arizona State University, Tempe

Keywords	Climate mitigation, carbon, greenhouse gas, climate feedbacks
Population (Metropolitan Region)	13,340,068 (U.S. Census Bureau, 2015)
Area (Metropolitan Region)	12,557 km ² (U.S. Census Bureau, 2010)
Income per capita	US\$56,180 (World Bank, 2017)
Climate zone	Csa – Temperate, dry summer, hot summer (Peel et al., 2007)

Urbanization has concentrated more than 50% of the global population, approximately 70% of fossil fuel carbon dioxide (CO₂) emissions, and a significant amount of anthropogenic methane (CH₄) into a small fraction of the Earth's land surface. Were they a single nation, the 50 largest cities would have collectively ranked as the third largest emitter of fossil fuel CO₂ after China and the United States in 2010 (World Bank, 2010). Carbon emissions from cities and their power plants are projected to undergo rapid change over the next two decades with cases of growth and stabilization. Cities are emerging as “first responders” for climate mitigation – with an increasing number of voluntary carbon stabilization programs in the largest cities as well as active exploration of linked sub-national carbon emissions trading systems. The ability to accurately assess and project the carbon trajectories of cities depends on improved understanding of the urban carbon cycle including interactions between the atmosphere, built systems, land, ecosystems, and aquatic systems.

The following key questions motivate urban carbon cycle studies in general (Hutyra et al., 2014):

1. What are the urban anthropogenic carbon fluxes? How are these fluxes and associated carbon pools changing in time and space? How are they likely to change in the future?
2. What are the primary causes for discrepancies between research-grade and regulatory or “self-reported” emission inventories? Can we reconcile “top-down” and “bottom-up” approaches to quantifying fossil fuel CO₂ emissions?
3. Can we attribute fluxes to their underlying processes and resolve emissions in space and time?
4. How are these emissions manifested across cities, and what are their sensitivities to the many controlling factors in different urban environments: geography, topography, climate, ecosystem type, socioeconomics, and engineering/technological factors? Are there emerging urban typologies for carbon emissions?
5. How do we apply natural science information on urban carbon flows to support and assess climate change policy options and assess efficacy?

Answering these questions is challenging given the paucity of urban-scale carbon flux data – emissions estimates at the scale of cities are often nonexistent or highly uncertain (NRC, 2010). The Los Angeles Megacities Carbon Project (<http://megacities.jpl.nasa.gov>) is one of several pilot projects currently under way with the goal of increasing the availability, fidelity, and policy relevance of urban carbon flux data and improving scientific understanding of the controlling processes.

The Megacities Carbon Project began as a partnership between U.S. and French scientists in 2010 to establish measurement networks, data assimilation, and analysis in the megacities of Los Angeles (Kort et al., 2013) and Paris (Breon et al., 2014). The team is working with collaborators in São Paulo, London, and other megacities to coordinate research and data sharing. In addition to advancing the state of the art and promoting technical capacity building, these and other related efforts seek to contribute to the formation of a *urban carbon typology* with biogeophysical and socioeconomic characteristics that represent the diversity of processes controlling carbon fluxes for the world's cities. The Megacities Carbon Project also serves as a pathfinder for a potential global urban carbon monitoring system, one combining surface and satellite observations (Duren and Miller, 2012).

For the Los Angeles project, measurements of CO₂, CH₄, and carbon monoxide (CO) atmospheric mixing ratios are collected continuously from a network of 15 monitoring stations located in and around the basin (see Case Study 2.2 Figure 1). A mix of in-situ and remote-sensing methods are used to track carbon in the planetary boundary layer and total atmospheric column (Wunch et al., 2009; Kort et al., 2013). The surface measurements are traceable to international standards using calibration gas tanks at each site – offering a transparent, consistent, and traceable mechanism for intercomparison. In some locations, air samples are collected in flasks and returned to a central facility for analysis of radioisotopes to disentangle fossil fuel and biogenic sources. Satellites such as the Japanese Space Agency's Greenhouse Gas Observing Satellite and NASA's Orbiting Carbon Observatory provide periodic total column CO₂ measurements for LA and other global megacities (Kort et al., 2012; Silva et al., 2013) that are validated with surface-based measurements in and around those cities. All of these atmospheric carbon measurements are combined with tracer transport models and meteorological data to generate “top-down” carbon flux estimates at the urban scale.

A high-resolution “bottom-up” fossil fuel CO₂ flux estimate has also been constructed for the LA megacity by researchers at Arizona State University and JPL using the “Hestia” methodology (Gurney et al., 2012). Hestia combines extensive data mining of public databases and a variety of model algorithms to estimate fossil fuel CO₂ fluxes at the building/street level every hour of the year. Among the data utilized are traffic volume measurements, census data, fuel statistics, tax assessor parcel data, hourly power plant emissions monitoring, and local air quality emissions reporting (e.g., Mendoza et al., 2013). The top-down and bottom-up datasets will be integrated with synthesis analysis, resulting in reduced uncertainty in carbon fluxes and improved understanding of the controlling processes. This information can help assess the impact of carbon management decisions including trends in emissions for specific municipalities, areas, and economic sectors. Improved understanding of the biogeophysical and socioeconomic processes that drive a city's carbon footprint and the linkages between them can help inform future projections and planning by urban stakeholders.



Case Study 2.2 Figure 1 Conceptual illustration of the tiered observational system applied by the Megacities Carbon Project in Los Angeles is also representative of elements found in other urban carbon studies.

Finally, a key goal of the Megacities Carbon Project is to deliver urban carbon data via a web-based portal for transparent data sharing. The objective is to provide decision-relevant carbon information to a broad range of stakeholders: urban planners, mayors, regional policy-makers, carbon markets, businesses, and

members of the general public. The concept is that pilot efforts that demonstrate voluntary data sharing between cities could reduce barriers to broader visibility into carbon emissions globally, thus enabling greater collective confidence in climate mitigation efforts.

The Los Angeles Megacities Carbon Project is funded by the U.S. National Institute of Standards and Technology (NIST), National Aeronautics and Space Administration (NASA), and National Oceanographic and Atmospheric Administration (NOAA) as well as contributions from the California Air Resources Board and the Keck Institute for Space Studies (KISS).

2.3.4 Urban Air Quality

With the confluence of rapid urbanization, fast-growing populations due to mass migration from rural areas, and industrialization since the mid-20th century, observed urban air quality has been declining (Kura et al., 2013). Not only does this confluence result in increased air pollution, it also threatens sustainable urban living and has negative health impacts. Urban air pollution is linked to about 1 million premature deaths and 1 million prenatal deaths each year (Kura et al., 2013). In addition, it is costly to ameliorate. It is estimated that developed countries spend about 2% of gross domestic product (GDP) on urban pollution, whereas developing countries spend about 5% of GDP for urban pollution (Kura et al., 2013).

Urban air quality varies regionally. Using satellite observations, Lamsal et al. (2013) showed that regional differences in industrial development, per capita emissions, and geography were related to the population–pollution relationship. The study showed that, for the same population, a developed city might experience six times the pollution concentration of a developing city. A satellite-based multipollutant index illustrates these differences, with cities exhibiting higher levels of individual pollutant types based on region (Cooper et al., 2012). An additional study in which a multipollutant index for cities was developed found Dhaka, Beijing, Cairo, and Karachi as cities with the poorest air quality (Gurjar et al., 2008).

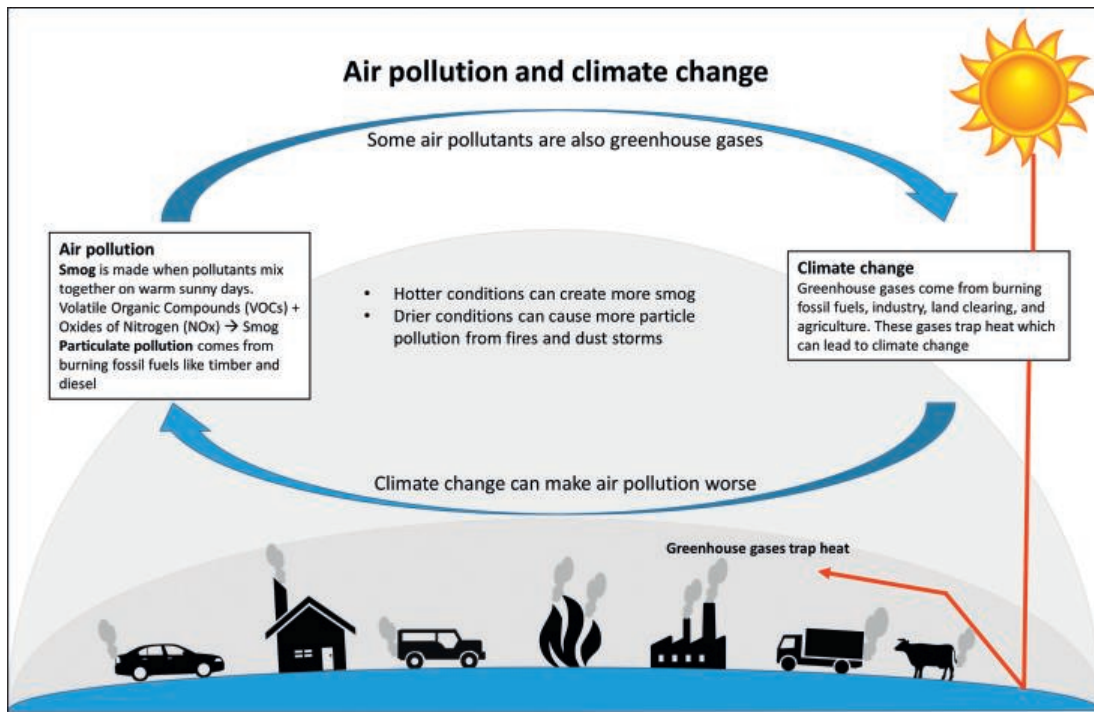


Figure 2.2 *The relationship between urban air pollution and climate change.*

Six main urban air pollutants are observed and measured: ground-level ozone, carbon monoxide, sulfur dioxide, particulate matter, lead, and nitrogen dioxide. Sources of these emissions include traffic, agriculture, fuel burning, natural sources (such as dust and salt), and industrial activities (see Figure 2.2). A recent study (Karagulian et al., 2015) found that for global particulate matter emissions, traffic is the largest source, followed by domestic fuel burning for cooking and heating. Looking specifically at emissions from vehicles, pollution concentrations can be directly correlated to daily rush hours and to the winter season. One study found that in Gothenberg, Germany, winter temperature inversions are associated with higher levels of traffic-related pollutants, including carbon monoxide, nitrous oxide, and nitrogen dioxide (Janhäll et al., 2006).

The spatially heterogeneous urban landscape with its inherently complex and highly variable emission sources makes both urban pollution measurement and modeling challenging endeavors. Zauli et al. (2004) reported that the spatial variability of pollution concentrations in cities often leads to mischaracterization of the urban environment and thereby complicates the study of the microclimate and its associated urban planetary boundary layer.

Climate change is projected to have impacts on the amounts of air pollutants and thus air quality in urban areas. Future changes are sensitive to both pollutant type and geographic region. The meteorological conditions (e.g., temperature inversions) that contribute to air quality in cities are also projected to change in the future (Jacob and Winner, 2009). Warming temperatures are linked to higher levels of ground-level ozone in many cities, and

ozone concentrations are projected to increase, particularly in the United States and Europe (Jacob and Winner, 2009; Katragkou et al., 2011). Future changes in particulate matter are less certain (Dawson et al., 2014).

Because they are prone to poor air quality, urban areas can invest in a variety of initiatives to have cleaner air. Pugh et al. (2012) showed that, along with controlling pollutant emissions and increasing dispersion (through changes in wind speed, wind direction, and atmospheric qualities), cities could improve air quality by increasing the deposition rates of pollutants. The study underscores the findings that green infrastructure (e.g., in urban street canyons) can be very effective deposition sites, reducing nitrogen dioxide (NO₂) by 40% and particulate matter by 60%. Along with other proven benefits to the urban center, particularly in the context of climate adaptation, vegetation can also be an efficient urban pollutant filter that helps to raise air quality at the street level in dense urban areas. For an example of the potential effectiveness of green infrastructure on reducing urban air pollution, a study of Toronto found that increasing the surface area for green roofs by 10–20% would greatly improve air quality in the city through pollutant removal (Currie and Bass, 2008).

To comprehensively study urban air quality in the context of climate change, an integrative strategy should include air quality measurements, which can be gathered through meteorological networks and satellites sensors, along with low-cost personal devices that can both collect and share real-time pollution data (Bertaccini et al., 2012). Emissions and pollutant data collected through urban observing networks can inform planning, thus allowing cities to be better able to issue air quality alerts. Such a system is already in

place in Santiago de Chile (Gramsch et al., 2006). In order to track how clean and green technologies and other strategies within the climate adaptation framework are impacting urban pollution, monitoring ambient air quality, source emissions, and indoor air quality is required. This could lead to improved modeling of emissions and atmospheric dispersion (Kura et al., 2013).

2.4 Natural Climate Variability

Variations in the climate due to natural processes influence urban climate risk. The effects from human activities on the climate system are superimposed on the background natural climate variability. This section introduces the major modes of variability and identifies some examples of how they affect the climate in certain cities. The predictability of these modes, which in some cases allows for advanced preparedness, can serve as a learning tool for planning for future climate changes.

By analyzing natural climate variability, scientists and urban decision-makers can improve responses to current climate hazards and vulnerabilities and prepare for future changes.

2.4.1 Overview

The major modes of natural climate variability include the El Niño Southern Oscillation (ENSO), the North Atlantic Oscillation (NAO), and the Madden-Julian Oscillation (MJO). Additional modes include the Pacific Decadal Oscillation (PDO), Atlantic Multi-Decadal Oscillation (AMO), Indian Ocean Dipole (IOD), and the Pacific North American pattern (PNA) (see Table 2.3). To varying degrees, these modes represent coupled interactions or feedbacks between the atmosphere and ocean and can be thought of as preferred patterns in space and time. These modes are characterized by indices that measure their phase and/or strength. The influence of each mode varies depending on the season of the year. A given city's

Table 2.3 Temporal and spatial scales of major modes of natural climate variability.

Mode & Acronym	Temporal scale	Spatial scale
El Niño Southern Oscillation (ENSO)	Typically occurs every 3–7 years. El Niño and La Niña events (opposite phases of ENSO) generally last 9–12 months. They develop during March–June, reach peak intensity during December–April.	Equatorial eastern and central Pacific Ocean, with effects on circulation seen in tropics. Teleconnections ^a span the globe, depending on phase and season.
Madden-Julian Oscillation (MJO)	Cycles every 30–60 days Greatest level of activity is during the late fall, winter, and early spring. MJO activity is enhanced in connection with the warm sea surface temperatures during an El Niño. Activity peaks before El Niño events, then is absent throughout its duration. MJO activity strengthens during La Niña (Seiki et al., 2015) Strong year-to-year variability.	Tropical regions, primarily over the Indian and Pacific Oceans. Can also be present in the tropical Atlantic and over Africa. Teleconnections span the globe, depending on phase and season.
North Atlantic Oscillation (NAO)	Exhibits considerable interseasonal and interannual variability, and prolonged periods (several months) of each phase of the pattern are common The wintertime NAO also exhibits significant multi-decadal variability	Atlantic Ocean, with one center located over Greenland and the other near the Azores. Teleconnections in the eastern United States, western Europe, and the Mediterranean
Pacific Decadal Oscillation (PDO)	Shifts between warm and cool phases occurs every 20–30 years (Mantua et al., 1997). Phases identified by prolonged sea surface temperature anomalies ^b in the equatorial and North Pacific.	Pacific Ocean Teleconnections in the United States and South America
Atlantic Multidecadal Oscillation (AMO)	The warm and cool phases of AMO persist for approximately 20–40 years due to changes in the overturning circulation of water and heat in the North Atlantic.	North Atlantic Ocean Teleconnections in North America and the United States
Pacific/North American Pattern (PNA)	Low-frequency mode that varies on interannual-to-decadal time scales. Strongly influenced by the dynamical processes of the NAO, reacting with Rossby waves coming from Asia (Baxter and Nigam, 2013).	Pacific Ocean through North America Associated with strong fluctuations in the strength and location of the East Asian jet stream.
Indian Ocean Dipole (IOD)	Aperiodic	Indian Ocean Teleconnections in Australia and other countries that surround the Indian Ocean basin

^a Teleconnections are linkages between weather and climate changes occurring in widely separated regions of the globe.

^b An anomaly is the difference of (usually) temperature or precipitation for a given region over a specified period from the long-term average value for the same region.

Box 2.2 Modes of Natural Climate Variability and Cities

EL NIÑO SOUTHERN OSCILLATION

El Niño (La Niña) episodes are characterized respectively by the warming (cooling) of the tropical central and eastern Pacific surface. The main atmospheric manifestation, known as the Southern Oscillation, is a seesaw pattern of the global-scale tropical and subtropical surface pressure, which also involves changes in the trade winds and tropical circulation and precipitation (Rasmusson and Wallace, 1983).

Cities impacted by El Niño (La Niña) events include Singapore (Earnest et al., 2012), Caracas (Bouma and Dye, 1997), and Nairobi (see Case Study 2.3).

NORTH ATLANTIC OSCILLATION

The North Atlantic Oscillation (NAO) is a quasi-regular variation of atmospheric pressure between subtropical and high latitudes (Hurrell et al., 2003). It is the dominant mode of atmospheric circulation variability in the North Atlantic region. Its influence on climate extends over a much larger region, from North America to Europe, Asia, Africa, and even more remote regions. The NAO and its influence are stronger in northern hemisphere winter, but are present throughout the

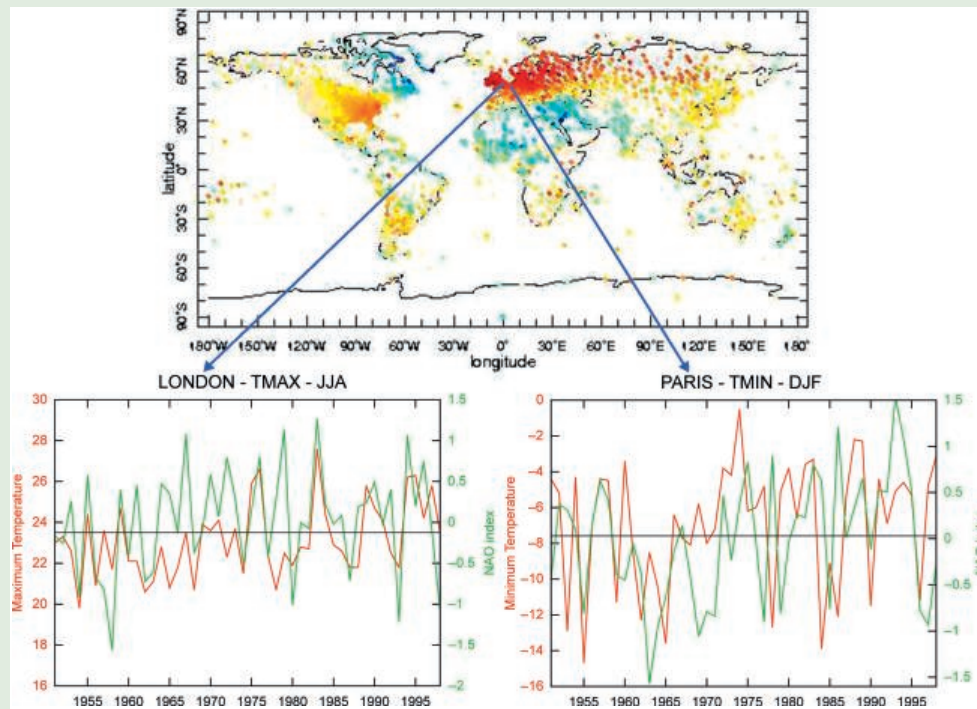
year. Although the NAO exhibits interannual variability, there has been a trend over approximately the past 30 years toward a more persistent positive state (Visbeck et al., 2001).

Examples of cities impacted by the North Atlantic Oscillation include Belgrade (Luković et al., 2015) and Oslo (Pozo-Vázquez, 2001). During the positive phase of the NAO, London and Paris generally experience warmer than average temperatures, while Athens is typically cooler than normal conditions (see Box 2.2 Figure 1).

MADDEN-JULIAN OSCILLATION

The Madden-Julian Oscillation (MJO) is the dominant mode of tropical intraseasonal climate variability (cycling every 30–60 days). It is a “pulse” of cloudiness and rainfall moving eastward in the equatorial region, in the Indian Ocean, and the western Pacific Ocean (Zhang, 2005), and it can excite atmospheric teleconnections that affect the climate and weather in many regions around the world.

Cities influenced by the MJO include Rio de Janeiro (see Case Study 2.3), Seattle (Bond and Vecchi, 2003), and Dakar (Conforth, 2013).



Box 2.2 Figure 1 The impacts of the NAO on surface temperature. The upper panel shows the correlation between the NAO index and winter surface temperature (from <http://www.ldeo.columbia.edu/res/pi/NAO/intro/correlations.html>). Areas in yellow and red (blue and green) indicate regions where a positive (negative) NAO index is linked with above (below) normal temperatures. The two graphs plot temperature against the NAO index in London (for summer maximum temperature) and Paris (for winter minimum temperatures). In both cities, London during the summer and Paris during the winter, warmer than normal temperatures (red line) are associated with positive NAO values (green line).

The cities provided here, as examples of those that are impacted by the major modes of natural variability, are a select group for each mode. A much larger number of cities across the globe, although not identified, may experience impacts of the different modes. The cities in Box 2.2 were chosen based on available literature documenting the relationships between their climate and natural variability.

Case Study 2.3 Rio de Janeiro Impacts of the Madden-Julian Oscillation

Alice Grimm

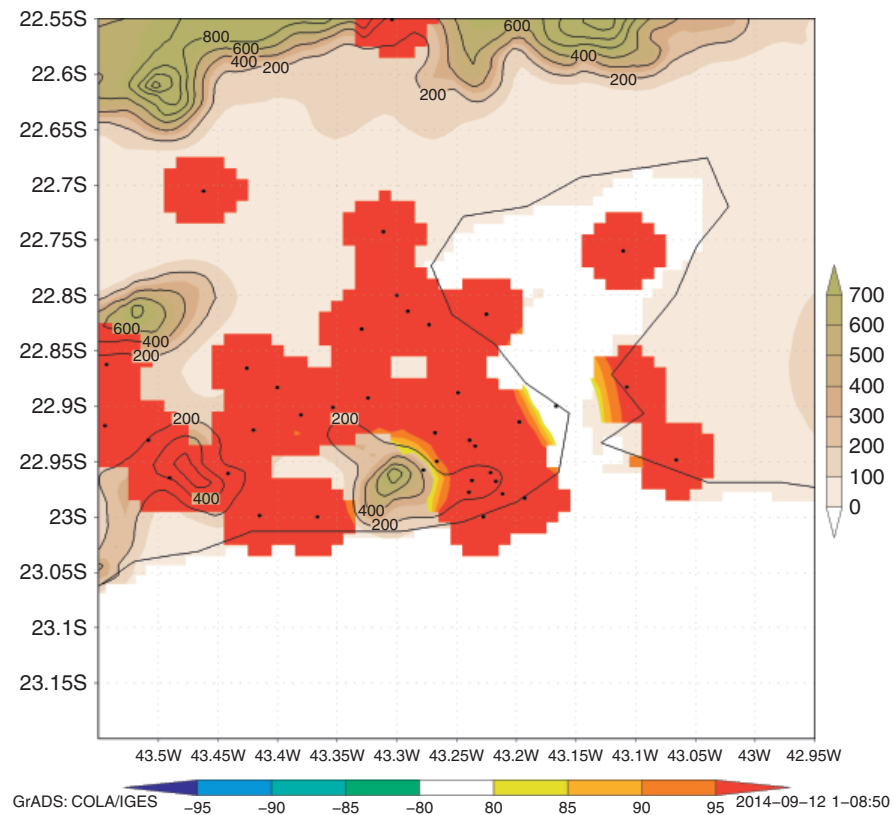
Federal University of Paraná, Curitiba

Keywords	Madden-Julian Oscillation, precipitation, rainstorm, disasters
Population (Metropolitan Region)	12,981,000 (UN, 2016)
Area (Metropolitan Region)	5,328.8 km ² (IBGE, 2015)
Income per capita	US\$8,840 (World Bank, 2017)
Climate zone	Am – Tropical monsoon (Peel et al., 2007)

characteristics of Rio de Janeiro's natural terrain, inadequate urban planning, and the city's sprawl over mountains and marshlands have made it prone to landslides and flooding. In the preceding century, one of the worst rainstorms happened in January 1966, when almost 250 millimeters of rain fell in less than 12 hours, causing loss of life and large economic damages (UEL, 2014; Corpo de Bombeiros, 2014). Another strong flood event happened in February 1988, when it rained over 430 millimeters over a 4-day period, killing 290 people and leaving close to 14,000 without homes (UEL, 2014; Corpo de Bombeiros, 2014; Costa, 2001; UNDRO, 1988). In the 21st century, the worst episode of floods and landslides in the metropolitan area occurred in April 2010, causing large-scale disruption to local livelihoods. Observations in the region near Rio de Janeiro show heavy rainfall events have been increasing over the past 50 years, creating a cause for concern and further analysis.

Rio's location within the South Atlantic Convergence Zone (SACZ)⁵ makes the city prone to intense rainfall events during the southern hemisphere summer (December-February) rainy season, beginning in spring and ending in autumn. Intense precipitation events in Rio de Janeiro are mainly caused by frontal systems and occurrence of the SACZ (Dereczynski et al., 2009). The frequency and intensity with which these large-scale

The metropolitan region of Rio de Janeiro, Brazil, including Niteroi and other neighboring cities with a total population of more than 11.8 million, is vulnerable to rainstorm-related disasters. The



Case Study 2.3 Figure 1 Meteorological stations used in Rio de Janeiro to assess the impact of MJO on the frequency of extreme events in summer (December, January, and February). Lines indicate topography (in meters), with the three massifs that surround the city (compact mountain groups). In the right half of the figure is the Bay of Guanabara and in the bottom is the Atlantic Ocean. The red color indicates the stations in which the number of extreme precipitation events significantly increases during Phase 1 of MJO in summer (level of confidence better than 95%).

⁵ The SACZ is a local maximum in cloudiness, precipitation, and low-level convergence that extends across southeastern Brazil and the western South Atlantic.

(synoptic) phenomena occur is modulated by climate variability, including El Niño and La Niña episodes in the inter-annual time scale, and the Madden-Julian Oscillation (MJO) in the intraseasonal time scale (Grimm and Tedeschi, 2009; Tedeschi et al., 2015; Hirata and Grimm, 2015). Although the ENSO influence is less consistent, the MJO impact is very significant. A statistical assessment of the connection between Phase 1 of MJO, when enhanced equatorial rainfall associated with the event is located over the western Indian Ocean and extreme precipitation (defined as above the 90th percentile), confirmed with 95% confidence level that in all but one series of station precipitation data analyzed in the city of Rio de Janeiro the number of extreme summer rainfall events increased during Phase 1 of MJO (see Case Study 2.3 Figure 1).

The MJO is not the sole contributor to or necessarily the main influence on the intensity and frequency of extreme precipitation

events in Rio de Janeiro. As a city near the sea and surrounded by mountains, there are also local effects (such as land and sea breezes) producing heavy rainfall, and there have been very extreme events not associated with MJO. However, the relationship between the MJO and intense precipitation may allow for, in some cases, advance planning in order to reduce climate risks. The MJO's level of predictability contributes to Rio de Janeiro's precipitation-based planning; knowledge of the patterns of the MJO can prove to be useful in infrastructural and flood contingency efforts at the local scale. By using regional climate models to simulate the cyclical influence of the MJO, a more accurate projection of future interannual variability in Rio de Janeiro rainfall can be provided. With damaging floods in recent memory for this urban setting, precipitation prediction is especially important to inform policies that contribute to proactive adaptation and resilience efforts aimed at protection of local and precipitation-vulnerable people and their livelihoods.

climate variability maybe influenced by a combination of patterns, although one may have a dominant influence and they could act at different timescales (see Case Study 2.3). Box 2.2 presents examples of cities impacted by modes of natural variability.

The modes of natural climate variability can affect not only monthly, seasonal, and annual mean temperature or precipitation totals, but can also (and even more significantly) affect the frequency and intensity of extreme events that can produce natural disasters (Grimm and Tedeschi, 2009). It is important for urban stakeholders to be aware of climatic modes and how they may impact key urban sectors and infrastructure (Ning and Bradbury, 2015).

Understanding how climate change may influence natural climate variability is an active area of research. Although the confidence in future climate projections on how patterns of natural variability may change in the future is low (see Section 2.4.3), some modes (such as ENSO and MJO) have predictability on season-to-annual timescales. This allows for their evolution to be forecasted in advance. Advanced lead-time to climate risks on these shorter timescales can help decision-makers prepare ahead for possible impacts. The lessons learned through preparedness for extreme events associated with natural variability can potentially be applied to the planning of adaptation and resilience strategies for future climate extremes.

2.4.2 Natural Climate Variability and Urban Decision-Making

The availability and dissemination of seasonal forecast information, based in part on the modes of natural climate variability, have the potential to inform decision-making in many urban areas. Known teleconnections between a mode and climate variable for a given city could aid planning and management of urban sectors, including public health, water resources, and energy. For example, if water managers in a particular city are anticipating a drier-than-normal-season

related to ENSO or the NAO, they might not release water from a dam even when faced with an immediate short-term risk of minor flooding so that water supplies remain adequate in the months to come. Droughts in Brazil, which can severely impact water supplies, have been linked to such patterns of natural climate variability (Marengo, 2004). Recognizing this relationship, utility managers in the river basin where the city of Rio de Janeiro's water supply comes from have developed new management practices (Formiga-Johnsson and Britto, 2009). Case Study 2.4 provides an illustration of how cities may prepare for climate extremes and health impacts associated with patterns of natural climate variability in part based on seasonal forecast information and how climate change may play a role (see Chapter 10, Urban Health).

Across Scandinavia, the NAO is linked to seasonal rainfall and therefore streamflow. This link in turn affects hydropower output (Cherry et al., 2005). In cities across the region (e.g., Copenhagen and Stockholm), this known relationship could allow for advanced planning in the energy sector, given that a seasonal forecast could be used to predict energy prices and estimate demand (see Chapter 12, Urban Energy).

Additionally, climate variability is often linked to water usage and supply (see Chapter 14, Urban Water Systems), which also presents opportunities for decision-making based on seasonal forecast information. In North America, Portland, Oregon demonstrates observed linkages between climate variability and water resources, illustrating the potential for forecasts to guide water resources management (Chang et al., 2014).

For an example in the public health sector, seasonal pollen in London has been linked to the phase of the NAO (Smith and Emberlin, 2006). Based on the state of this mode of natural variability, health officials can potentially have lead-time to preparing for high-impact events for allergy sufferers (see Chapter 10, Urban Health). Urban air quality in Hong Kong has also been linked to El Niño phases (Kim et al., 2013).

Case Study 2.4 Will Climate Change Induce Malaria in Nairobi?

Annie Ramsell

Climate Change Adaptation Unit, UNEP, Nairobi

Keywords	Climate science, malaria, El Niño, urban health, rainfall, science for cities, action plan
Population (Metropolitan Region)	6,547,547 (KNBS, 2010)
Area (Metropolitan Region)	30,389 km ² (KNBS, 2010)
Income per capita	US\$1,380 (World Bank, 2017)
Climate zone	Cwb – Temperate, dry winter, warm (Peel et al., 2007)

Kenya's capital city, Nairobi, is projected to be adversely affected by the impacts of climate change, with temperature and rainfall variability resulting in an array of cross-sectoral climate-related impacts (IPCC, 2013). The shifting climatic system of the South Indian Ocean Dipole (IOD) is believed to contribute to the increasing uncertainty of seasonal and interseasonal rainfall and spatial variability in Kenya (IPCC, 2013; Hashizume et al., 2012) and is already leading to a warmer climate in Nairobi. These changes in climate are thought to make highland areas in East Africa more suitable for malaria epidemics, potentially placing Nairobi as a future "at risk" city for malaria (Ermer et al., 2012). Improved knowledge of malaria threshold conditions and greater predictability of localized weather patterns would enable the Government of Nairobi to assess the threat of a malaria epidemic and determine the need for a response strategy.

The IOD is a coupled ocean-atmosphere phenomenon in the equatorial Indian Ocean defined as the difference between the sea surface temperature (SST) of the eastern and western parts of the Indian Ocean and is measured by the Dipole Mode Index (DMI). A negative IOD event is characterized by cooler than normal water in the tropical eastern part of the Indian Ocean and warmer than normal water in the western part of the Indian Ocean basin. Heavy and prolonged rains during the short rainy season (September, October, and November) in the East African highlands are most likely influenced by positive IOD events (Hashizume et al., 2012). Any prolonged short-rains season is therefore conducive to a seasonal malaria event since the short-rains season is followed by warm weather, enhancing the development of mosquitoes and malaria parasites. A shift in the IOD induced by climate change could therefore directly influence the weather in Nairobi, exposing the city to future malaria epidemics. Even if precipitation and the IOD remained unchanged, warmer temperatures thereafter due to climate change could also increase malaria risk.

According to the Intergovernmental Panel on Climate Change (IPCC) Fifth Assessment Report (AR5; Smith et al., 2014), highland areas in East Africa could experience increased malaria epidemics due to climate change. However, the complexity of malaria development and how it is affected by climate variations is a subject of uncertainty. Nonetheless, theories on malaria thresholds have been studied and observed (Cox et al., 1999), and thresholds

Case Study 2.4 Table 1 Summary of Climate Variables for Kericho and Nairobi.

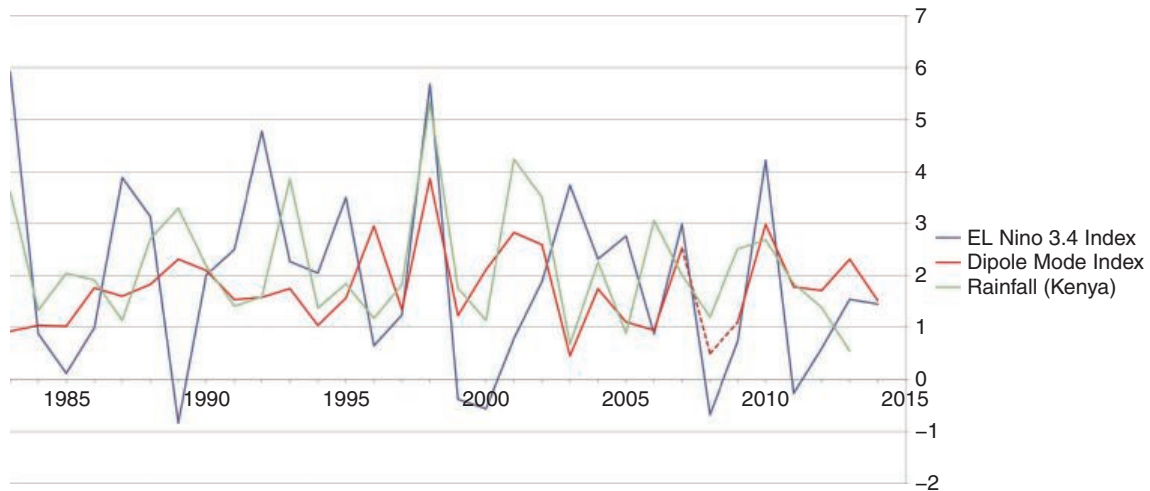
Climate variable	Minimum malaria threshold	Kericho (2,182 m)	Nairobi (198 m)
Precipitation	Greater than 80 mm for 5 consecutive months	✓	X
Relative humidity	Greater than 60%	✓	✓
Mean temperature	Greater than 14.5°C	✓	✓

for malaria transmission have been established for temperature, humidity, and precipitation. Malaria transmission requires a relative humidity of minimum 60%, monthly average precipitation of 80 millimeters or more for 5 consecutive months (Cox et al., 1999), and for the malaria development cycle to be completed at monthly mean temperatures not below 14.5°C and 20°C for the parasites *Plasmodium vivax* and *P. falciparum*, respectively (Kim et al., 2012).

Malaria epidemics have long been common in the Kericho district in western Kenya, and malaria is now a seasonal occurrence within the district. High levels of malaria incidence emerge in Kericho after the long rains in March until the declining temperatures decrease the transmission in July. Changes in climate variability, increased resistance to antimalarial drugs, population movements, alterations in mosquito vectors (e.g., species), and impaired health services are all contributing factors to the re-emergence of malaria seasonality in Kericho (Shanks et al., 2005). Many studies have implied that Nairobi is malaria-free because of its location at an altitude of 1,798 meters and its resulting low mean temperature (Hay et al., 2002). However, Kericho, at 2,182 meters, is situated at a higher altitude than Nairobi and its mean monthly minimum temperatures are not significantly different. Because temperatures alone do not correlate with malaria transmission and minimum humidity and precipitation are also required (Cox et al., 1999), an assessment of data on precipitation, temperature, and humidity in Nairobi and Kericho from Kenya Meteorological Services (KMS) assessed the climatic differences related to malaria transmission between these two sites. These findings are summarized in Case Study 2.4 Table 1.

Prolonged short-rain seasons are recognized as triggers for increased malaria transmission in the East African Highlands region (Hashizume et al., 2012), and, as such, the primary focus on potential malaria introduction in Nairobi was assessing data on the short-rains season precipitation and timeline. Data on monthly precipitation over a 30-year period show that Nairobi does receive the minimum 80 millimeters precipitation during its short-rains season, but the season has not exceeded 5 consecutive months in current conditions.

In the comparison site of Kericho, the data revealed that although moderate malaria transmission occurs throughout the year, including the short-rains season, the highest levels of malaria transmission were actually found to occur during the long rains (Tonui et al., 2013). The study subsequently looked into whether malaria-suitable climate conditions occurred in Nairobi during any period of the year. The data revealed that Nairobi had precipitation of 80 millimeters or



Case Study 2.4 Figure 1 Average rainfall over Kenya from eight weather stations for the period of December, January, and February (DJF) annually from 1983 to 2013, against sea surface temperatures (SSTs) in the central Pacific Ocean region associated with the El Niño Southern Oscillation (ENSO 3.4) and the Indian Ocean Dipole (IOD) (represented by the Dipole Mode Index) for the same periods.

more for only 4 consecutive months six times in the past 30 years. The observations show that the trigger point for malaria in Nairobi is increased precipitation, but no indication of increased precipitation for 5 consecutive months has been found in the past 30 years. Furthermore, extrapolating the precipitation trends to 2030 does not indicate that any malaria introduction will occur in Nairobi up to this future period.

This study shows that Nairobi is malaria-free because it does not meet the malaria threshold of more than 80 millimeters of precipitation over 5 consecutive months. Nevertheless, Nairobi was found to be very close to meeting all minimum thresholds. When correlating the precipitation data with El Niño events, the results show that 4 out of the 6 years in which Nairobi had 4 consecutive months of more than 80 millimeters precipitation are directly correlated to El Niño events. Nairobi is therefore only 1 month short from being climatically suitable for malaria during years with El Niño events. This indicates the need for better climate variability modeling in Nairobi so it will have the capacity to

project potential future outbreaks of malaria. This will make the city more resilient in preparing for effective preventative malaria response action.

Rainfall in East Africa is known to align closely with the ocean-atmospheric anomaly of the El Niño Southern Oscillation (ENSO) over the Pacific Ocean, reacting as well with the IOD in the Indian Ocean, as Case Study 2.4 Figure 1 demonstrates. The effect, known as a teleconnection, refers to climate anomalies that are related to one another over large distances. The 2014 IPCC AR5 indicates that future warming is highly likely to intensify interannual rainfall variability in East Africa, resulting in an increase in the number of extremely wet seasons (Smith et al., 2014). Monitoring and prediction of ENSO are therefore of large value for countries in the East Africa region.

In conclusion, improved climate modeling and monitoring of future El Niño events will enable the city government to plan for and reduce the potential impacts of future malaria epidemics in Nairobi.

It is important to recognize that despite the connections between natural variability and sectoral impacts, there are many other factors involved, and climate may not be the sole or best predictor of societal impacts. For example, in Phoenix, Arizona, although water usage is linked to climate variables (temperature and precipitation), using local observations does not necessarily aid managers because the water supplies are located far outside of the city (Balling and Gober, 2007). Furthermore, every occurrence of a particular mode of natural variability may not bring the expected impacts due to differences across the events themselves. Therefore, decision-making based on climate variability is constrained by uncertainty. However, these opportunities do illustrate that modes of natural variability do impact cities, and decision-making can take short-term seasonal information into account along with other factors. This is similar to the process of using future climate risk data in long-term planning.

Even if modes of variability and teleconnections remain the same, climate change could modify their impacts (see Section 2.4.3). For example, if climate change leads to a drier mean state in southern California, El Niño-driven precipitation events might be less likely to lead to saturated ground, reservoirs, and flooding. Alternatively, the same drier mean state could be associated with more fires and changes in vegetation cover that paradoxically increase flood risk once El Niño rains arrive.

The potential for and current use of scientific information in decision-making demonstrates the need for continuing interactions between scientists and stakeholders and also emphasizes the need for improved communication of scientific information. Research on the effectiveness of seasonal forecasts for planning has identified a set of constraints limiting the usefulness

of the information and proposed ways to overcome them (Patt and Gwata, 2002). Scientists must incorporate the needs of the local users, clearly communicate uncertainties, and repeat the process regularly. These barriers and ways to overcome them were tested at rural sites in Zimbabwe; the outcomes may have application to many cities in the developing world (Patt and Gwata, 2002).

2.4.3 Modes of Natural Variability and Climate Change

Interactions between climate change and natural climate variability are complex and their predictability remains challenging. As decision-makers in cities become more familiar with using seasonal forecast information, clear expression of how these modes may change in the future will become increasingly important (Deser et al., 2012). As the climate changes globally, there may be changes in patterns of natural variability in terms of their strength, frequency, and the duration of the various modes. Even if the patterns of variability remain similar to what they are today, climate change may alter the background (or “mean state”) thereby modifying teleconnection patterns that drive regional climate impacts. This could have implications for cities, especially those that use seasonal information for planning.

The Intergovernmental Panel on Climate Change (IPCC) Fifth Assessment Report (AR5) found that El Niño is projected to continue to remain the most prominent mode of natural variability and will continue to have global influences (Christensen et al., 2013). It remains uncertain as to whether a more El-Niño-like state due to warmer sea surface temperatures will become more dominant than La Niña with climate change (Collins et al., 2005). As for the frequency of El Niño events with climate change, Cai et al. (2014) project a doubling in occurrences of El Niño with climate warming, stemming from projected warming over the eastern equatorial Pacific Ocean. Other studies (e.g., Collins et al., 2010) suggest that it is not possible to project changes in El Niño frequency at this time.

The teleconnections associated with El Niño that may impact regional climate and thereby cities, may also change in the future. An eastward shift in the Pacific-North American (PNA) pattern is projected, and this shift may intensify rainfall anomalies along the west coast of North America and push El Niño-associated warming further east across the continent (Zhou et al., 2014). Cities potentially impacted by such changes include Seattle and Los Angeles. Precipitation at the regional scale associated with El Niño events is likely to intensify due to changes in available moisture (Christensen et al., 2013; Power et al., 2013).

The NAO is projected to become (on average) slightly more positive with climate change caused by increasing greenhouse

gases (GHGs), with continuing large natural variations, as observed in the present climate (IPCC, 2013). A more positive NAO could be associated with wetter conditions in northern Europe, drier conditions in the Mediterranean, and fewer cold air outbreaks over eastern North America. Future projections of the NAO are highly sensitive to the climate models used because some are unable to simulate this pattern of observed variability in the present climate (Davini and Cagnazzo, 2014). Despite these difficulties, some climate models are able to simulate current and future teleconnections from the NAO with regard to temperature and precipitation in the United States (Ning and Bradley, 2015).

2.5 Observed Climate in Cities

Observations over the past century at the global and continental scales have shown that climate is already changing in response to increasing GHG concentrations. Global temperatures and sea levels have both been rising. Regionally, changes in both mean climate variables (e.g., seasonal and annual temperature and precipitation) and the frequency and intensity of extreme events (e.g., hot and cold days, days with intense precipitation, coastal storms, and floods) have been observed (IPCC, 2012; 2013). The climate in many cities is also changing, but attributing urban climate change to increasing GHG emissions is challenging because of the process of urbanization and its connection to the urban heat island effect (see Section 2.3.1) and the relatively small scale of analysis that increases variability. In many cases, changes observed in cities across the globe may serve as a starting point for identifying the climate risks that may increase in the future.

Attributing observed trends to natural and/or anthropogenic processes is a major focus of climate science study (Cramer et al., 2014). There is considerable scientific consensus that the observed warming trends in recent decades cannot be explained without anthropogenic forcing (IPCC, 2013). In contrast, recent changes in regional precipitation patterns may be more heavily driven by natural climate cycles (Hoerling et al., 2010). To better understand how the climate of urban environments is changing and how this relates to the process of urbanization, long-term climate data records are required, reinforcing the need for improved observations.

2.5.1 Urban Climate Trends

Across the globe, annual average temperature (combined land and ocean surface data) has increased by approximately 0.85°C since 1880 (IPCC, 2013). Global sea levels have also risen, with a rate of 1.2 mm/year for the 1901–1990 period and an increased rate of 3.0 mm/year for the 1993–2010 period (Hay et al., 2015). Although these trends

are global, warming temperatures and rising sea levels have been observed in numerous cities (Blake et al., 2011). Documented climate trends also encompass high and low temperature extremes, heat waves, intense precipitation, and coastal flooding in many cities (Alexander et al., 2006; Mishra and Lettenmaier, 2011).

In one study of 217 urban areas across the globe, researchers found that these areas have experienced significant increases in the number of heat waves (defined as periods during which the daily maximum temperature stayed above

the empirical 99th percentile consecutively for six or more days) in the past 40 years, whereas cold wave frequency (periods during which the daily maximum temperature stayed below the empirical 99th percentile consecutively for six or more days) has decreased (Mishra et al., 2015). This study also found that the number of hot days and hot nights (defined in as the 99th percentile of daily maximum and minimum temperatures, respectively) also increased in the majority of cities analyzed (see Case Study 2.5). A smaller number of cities showed an upward trend in extreme precipitation, and some cities showed significant downward extreme

Case Study 2.5 Climate Extreme Trends in Seoul

Yeonjoo Kim and Won-Tae Kwon

Yonsei University, Seoul

Keywords	Temperature extremes, coastal flooding, public health
Population (Metropolitan Region)	23,575,000 (Demographia, 2016)
Area (Metropolitan Region)	2,590 km ² (Demographia, 2016)
Income per capita	US\$27,600 (World Bank, 2017)
Climate zone	Dfa – Cold, without dry season, hot summer (Peel et al., 2007)

Seoul, South Korea has a temperate climate with four seasons and a relatively large temperature difference between the hottest days of summer and the coldest days of winter. It experiences hot, humid weather in the summer under the influence of the North Pacific high-pressure system and cold weather in the winter under the influence of the Siberian high-pressure system. The summer climate in Seoul is linked to the East Asian monsoon, a pattern of natural climate variability with connections to the Madden-Julian oscillation (Chi et al., 2014).

Temperatures from 1908 to 2013 were investigated with a focus on extremes. Averages of mean, minimum, and maximum temperatures all show increasing trends over the past 106 years. In particular, the minimum temperature during the winter increased at an average rate of 0.5°C/decade.

Temperature-related extremes – tropical days⁶, tropical nights⁷, and frost days⁸ – were investigated. Results show that Seoul has been experiencing changes in extreme temperatures. In particular, the increase in the number of tropical nights is very significant, which can adversely affect human health and energy demand. Warmer nighttime temperatures may result in increased air conditioning usage, placing strain on energy supplies. Increasing nighttime temperatures may also impact vulnerable populations, such as the elderly, children, and those with pre-existing medical conditions.

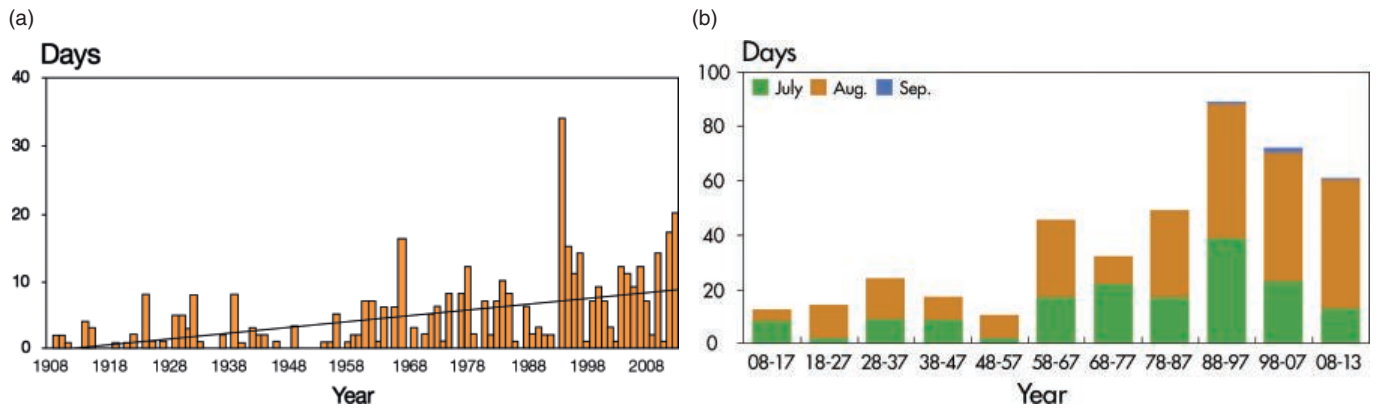
Seoul experienced an average of 35.7 tropical days per year over the past century, with a slight decreasing trend of –0.6 days/decade, which is not statistically significant. For tropical nights, the average is 4.2 days per year, and there is a strong increasing trend with a rate of 0.9 days/decade (Case Study 2.5 Fig. 1). This trend reflects the fact that the minimum temperature during the summer has increased over the past 106 years at an average rate of 0.2°C/decade. Seoul experienced an average of 1.7 tropical nights for the earliest decadal period of the data record (1908–1957) and 6.2 days, a 600% increase, for the latest period analyzed (1958–2013). In 1994, the most frequent tropical nights (34 days), took place followed by 20 and 17 days in 2013 and 2012, respectively.

Seoul experienced an average of 107.9 frost days per year, with a decreasing trend of –4.5 days/decade (Case Study 2.5 Figure 2). For the 1908–1917 period, an average of 127.54 frost days was found, whereas for 2008–2013, an average of 95.5 days was observed. For the past 106 years, the minimum temperature during the winter showed marked increase of 0.5°C/decade, and such an increase was also present during the spring and fall. The largest drops in the annual frost days were found in March and November in Seoul. In March, an average of 22.3 days for the 1908–1917 period was found, compared to 11.8 days for the 2008–2013 period.

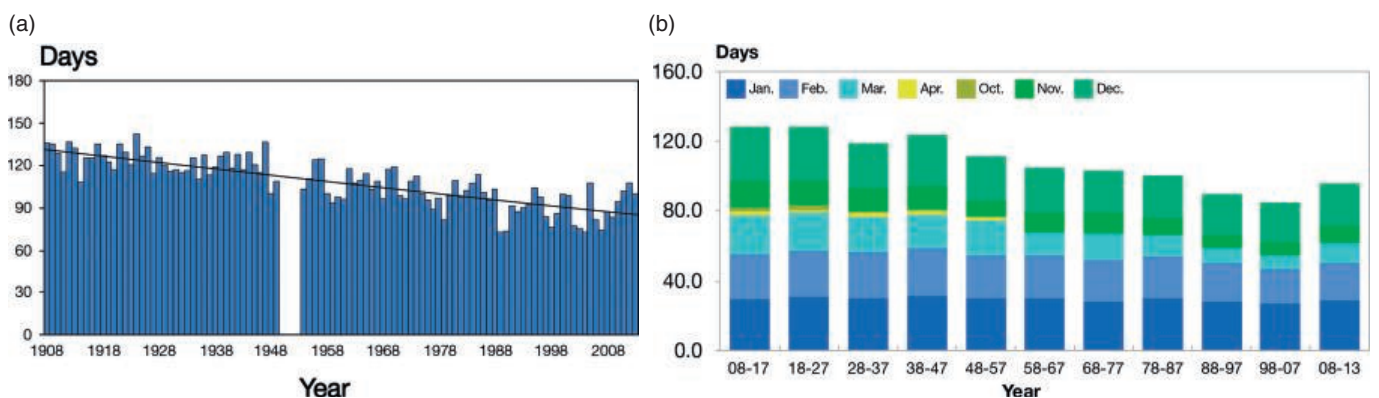
The recent observed trends are an example of how trends in extreme temperatures can influence urban decision-making. In Seoul, based on the climate data analysis, planning for an increased number of heat-related impacts in the health, energy, and other urban sectors may need to be considered.

Given anticipated increases in the frequency, duration, and intensity of heat waves due to climate change, Son et al. (2012) examined mortality from heat waves for 2000 through 2007. Heat waves are defined as two or more consecutive days with daily mean temperature at or above the 98th percentile for the warm season and mortality during heatwave days and non-heatwave days are compared. A significant increase in total mortality in Seoul was noted on heatwave days compared with non-heatwave days (8.4%; 95% confidence interval [CI]: 0.1%, 17.3%). As an additional analysis for the timing of the heatwave in the season, we compared mortality risk based on whether a

6 Tropical days are defined as days where daily maximum temperature exceeds 30°C.
 7 Tropical nights are defined as days where the daily minimum temperature exceeds 25°C.
 8 Frost days are defined as days where the daily minimum temperature falls below 0°C.



Case Study 2.5 Figure 1 Tropical nights in Seoul.



Case Study 2.5 Figure 2 Frost days in Seoul.

heatwave was the first in its summer in Seoul. The first heatwave of the summer had a larger estimated mortality effect than did later heatwaves.

Seoul has also been experiencing the urban heat island effect (UHI). Based on investigating near-surface air temperature data measured at automatic weather stations (AWSs) (Kim and Baik, 2005), the Seoul urban heat island deviates considerably from an idealized, concentric heat island pattern. This is attributed to the location of the main commercial and industrial sectors and the local topography. The temperature anomaly in southwestern and

southeastern Seoul is positive and its magnitude is large because these two regions have been built up for the two decades before 2001. It clearly shows increases in near-surface air temperature due to urbanization and industrialization. Furthermore, Lee and Baik (2010) performed statistical analysis of UHI intensity in Seoul, showing that the seasonal mean of UHI intensity is strongest in autumn and weakest in summer. The daily maximum UHI intensity is observed around midnight in all seasons except in winter, when the maximum occurrence frequency is around 08 LST, suggesting that anthropogenic heating contributes to the UHI in the cold season.

precipitation trends. Such events can have significant impacts on cities across multiple urban sectors. The results of Mishra et al. (2015) are similar to the observed changes found at the global scale in the IPCC Special Report on Extreme Events (IPCC, 2012).

2.5.2 Influences of Urbanization

How the UHI influences observed temperature trends globally (Parker, 2006; Hansen et al., 2010) and regionally (Arnfield, 2003; Peterson, 2003; Stone, 2007) is a focus of current research. While the UHI effect may have an influence on larger geographic scales (Stone, 2009), the IPCC

Fourth Assessment Report (Trenberth et al., 2007) states that the contribution of urbanization on global temperature trends is not significant, and any urban-related trend is an order of magnitude smaller than decadal and longer time-series trends. Similar results were presented in the IPCC Fifth Assessment Report (IPCC, 2013), which again found that the UHI effect has very limited influence on global temperature trends; however, the IPCC AR5 found that the influence on regional trends could be substantially larger (IPCC, 2013).

At the regional scale, some studies show that a percentage of the warming trends in cities can be linked to UHI effects, with estimates attributing nearly half of the observed decrease

in diurnal temperatures range for stations in the United States to urbanization and land-use change (Kalnay and Cai, 2003). Hausfather et al. (2013) found that urbanization accounted for between 14% and 21% of the increase in minimum temperatures since 1895 and for 6% to 9% since 1960 for stations within the United States. In New York, it is estimated that approximately one-third of the warming experienced in New York from 1900 to 2002 can be attributed to the UHI (Gaffin et al., 2008). An analysis of five North American cities found that one metric to measure the effects of increasing urbanization on temperatures in cities is the day-to-day variability in maximum and minimum temperatures (Tam et al., 2015).

Land-use and the UHI have contributed to the warming trend in Glasgow, which presents an interesting case because the temperatures increased as the population of the city decreased (Emmanuel and Kruger, 2012). Despite the falling population, the UHI persists because much of the urban infrastructure and land use changes caused by past growth remain in place.

Similar results have been found for cities in east China (Yang et al., 2011), most notably in the Yangtze River Delta, where the highest level of urbanization has occurred. Densely populated metropolis cities in this region have warmed 0.285°C per decade more than rural areas, which see fewer impacts from urban-related warming. From 1981 to 2007, an increase in annual mean temperature over east China of 0.578°C per decade was observed. Specifically, within the city of Shanghai, this trend amounted to 0.961°C per decade. Through comparison with rural sites and reanalysis of temperature data, approximately one-quarter of the observed warming trend is attributable to urbanization and changes in land use.

Although urbanization may be contributing to warming trends within cities, some studies have shown that rates of observed warming do not significantly differ from the trends observed in more rural locations. Adjusting global temperature data to remove the impacts of urban effects revealed that for 42% of global stations, urban areas warmed at slower rates compared to the surrounding non-urban areas (Hansen et al., 2001). Although the raw data showed that large urban areas experienced 0.25°C warming in the 20th century, this urban effect is largely influenced by regional temperature variability, errors in measurement, and nonuniformity of the station data. In London and Vienna, where both cities observed temperature records display the influence of the UHI, rates of warming are comparable between the city and the surrounding rural locations (Jones et al., 2008).

2.6 Future Climate Projections

Future climate scenarios can be used to inform resiliency efforts in cities. This section discusses available climate risk information at the city scale and presents examples of where it has been used to implement adaptation strategies. It is important to develop a process by which local, national, and international

researchers provide climate risk information to urban stakeholders and to ensure that the data are periodically updated through time. Regular updates are necessary to incorporate the latest climate science research available, including new models and methodologies, which are also described here.

2.6.1 Developing Climate Projections for Cities

Several steps can be followed to develop climate projections that can be used by cities as they plan and implement adaptation and mitigation strategies. A useful first step can be to scope out the main climate risk factors for cities; this is the subset of climate hazards that is of most consequence for a given city. This subset of hazards is selected on the basis of interactions between researchers and stakeholders and of expert judgment using quantitative and qualitative climate hazard information. Risk factors are generalized climate variables prioritized by consideration of their potential importance for a city. Quantitative (where possible) and qualitative statements of the likelihood of occurrence of these tailored climate risk factors, their potential impacts and their consequences are presented. Examples of climate risk factors include heat waves, coastal floods, intense precipitation events, and droughts, all of which can impact urban areas.

After initial scoping using climate risk factors, downscaled climate projections can be developed for cities. Global climate models (GCMs) and regional climate models (RCMs) are both tools that scientists use to project future climate at the local scale. GCM results are often statistically downscaled to provide information at higher spatial resolution. This is less common with RCMs, which are already downscaled dynamically. These techniques have advantages and disadvantages compared to each other (see Table 2.4 and Box 2.3), with the climate projections from both suitable to be incorporated into climate risk information for development of urban adaptation strategies, accompanied by a clear presentation of uncertainty (see Section 2.6.4) (Vaughan, 2016).

By incorporating the latest climate model outputs from the Coupled Model Intercomparison Project Phase 5⁹ (CMIP5; Taylor et al., 2012), prepared for the IPCC Fifth Assessment Report (IPCC, 2013), projections can be provided for more detailed model-based probability distributions of climate variables. Using a combination of climate models and representation concentration pathways (RCPs; Moss et al., 2010) linked to possible future GHG concentrations produces a matrix of outputs for a given climate variable (see Box 2.3). This allows, for each time period, a model-based range of outcomes (i.e., a distribution that shows for any given threshold the number of climate models and RCP results that are at, above, or below the threshold) that can be used to inform risk-based decision-making. The presentation of such model-based outcomes to stakeholders should include clear statements about associated uncertainties, which include uncertainties in future GHG emissions and how the climate system will respond, natural climate variability, local processes not captured by the climate models, and the increase in uncertainty with spatial resolution (Willows et al., 2003).

9 CMIP provides a framework for standard protocols and comparison in global climate modeling, and the outputs are used in the IPCC assessments.

Table 2.4 Comparison of Global Climate Models and Regional Climate Models for Downscaling for Urban Areas.

	Global Climate Models (GCMs)	Regional Climate Models (RCMs)
Resolution (spatial and temporal)	GCMs have coarse horizontal resolution of approximately 30 to 65 km. Outputs range from 3-hourly to monthly; preferred for use on longer timescales.	RCM resolution is generally on the order of 25–50 km. Outputs range from hourly to monthly; preferred for use on shorter timescales.
Computational power	GCMs are less computationally intensive.	RCMs are more computationally intensive.
Downscaling considerations	GCMs depict relevant large-scale climate phenomena (e.g., synoptic weather patterns) that impact the local climate of interest.	Regional phenomena such as orography and land use are incorporated in order to determine local climate impacts.
Requirements	High-quality historical climate data are required for bias-correction and statistical downscaling approaches with GCMs.	GCM boundary conditions are used as input for temperature and wind factors; without high-quality inputs, RCMs are limited.
Urban applications	GCM outputs can be downscaled for resiliency planning at metropolitan region scales	RCMs are able to simulate components of the urban climate system. Projections from RCMs can be used for resiliency planning.
Examples	Coupled Model Intercomparison Project Phase 5 (CMIP5; Taylor et al., 2012),	North American Regional Climate Change Assessment Program (NARCCAP; Mearns et al., 2009)

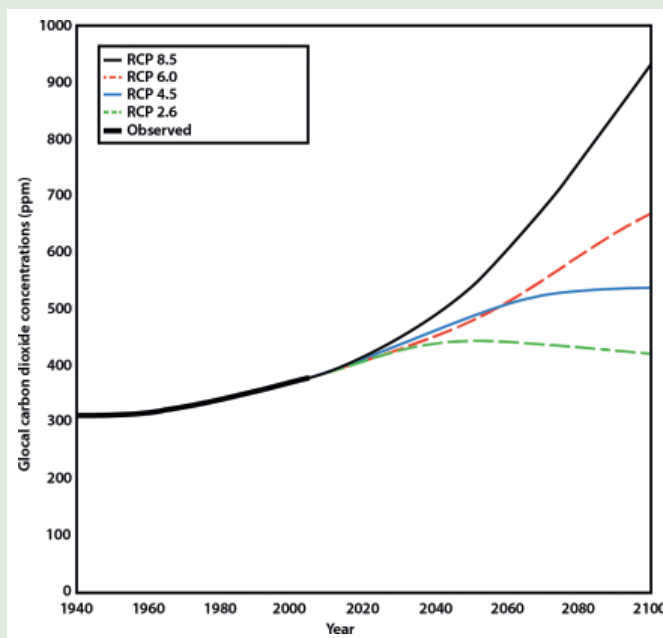
Box 2.3 Climate Models and Representative Concentration Pathways

Global climate models (GCMs) are physics-based mathematical representations of the Earth's climate system over time that can be used to estimate the sensitivity of the climate system to changes in atmospheric concentrations of greenhouse gases (GHGs) and aerosols.

Regional climate models (RCMs) are similar to GCMs, with the primary difference being that regional models are run at a higher spatial resolution that allows for the use of more detailed physical parameterizations to simulate certain processes such as convective precipitation, sea breezes, or differences in elevation.

Representation concentration pathways (RCPs) represent the amount of radiative forcing (measured in watts per meter squared) caused by GHGs and other important agents such as aerosols over time. Each RCP is consistent with a trajectory of GHG emissions, aerosols, and land-use changes developed for the climate modeling community as a basis for long- and near-term climate modeling experiments. RCPs serve as inputs to global climate models, in order to project the effects of these climate drivers on future climate.

Projections for temperature, precipitation, and sea level for *Second Urban Climate Change Research Network Assessment Report on Climate Change and Cities (ARC3.2)* were generated from IPCC Coupled Model Intercomparison Project Phase 5 (CMIP5) GCM simulations based on two RCPs (Moss et al., 2010). The analysis uses two RCPs, RCP 4.5 and RCP 8.5, which represent relatively low and high GHG projections and radiative forcing, respectively.¹⁰



Box 2.3 Figure 1 Observed CO_2 concentrations through 2005 and future CO_2 concentrations consistent with four representative concentration pathways (RCPs). Urban Climate Change Regional Network (UCCRN) climate projections are based on RCP 4.5 and RCP 8.5. Carbon dioxide and other greenhouse gas concentrations are driven by a range of factors, including carbon intensity of energy used, population and economic growth, and diffusion and adoption of new technologies, including energy efficiency and green energy.

Source: NPCC, 2015

¹⁰ The Paris Agreement in December 2015 set the goal of limiting global temperatures from increasing more than 2°C above pre-industrial levels by the year 2100, with an additional aim for an even more ambitious stabilization target of 1.5°C. Therefore, inclusion of additional RCPs, such as RCP 2.6, may be of greater importance for future climate projections.

2.6.2 Temperature and Precipitation

Climate projections for temperature and precipitation developed for the *Second Urban Climate Change Research Network Assessment Report on Climate Change and Cities (ARC3.2)* are based on downscaled climate data from Coupled Model Intercomparison Project Phase 5 (CMIP5) multimodel data set (see Annex 2, Climate Projections for ARC3.2 Cities). Projections were obtained for 35 GCMs used in the IPCC AR5. Local projections for 153 ARC3.2 cities are based on GCM output from the single land-based model grid box centered over each of the cities and is used to develop city-specific climate change projections for temperature and precipitation.¹¹ Projections are based on two RCPs, RCP4.5 and RCP8.5. See Annex 2 in this volume for the full set of projections for the 153 ARC3.2 Cities.

Although it is not possible to predict the temperature or precipitation for a particular day, month, or year, GCMs are valuable tools for projecting the likely range of changes over multidecadal time periods. These projections, known as *timeslices*, are expressed relative to the 1971–2000 baseline period. The 30-year timeslices are centered on a given decade. For example, the 2050s timeslice refers to the period from 2040 to 2069.

The projections for temperature and precipitation are provided for a set of cities across five geographic regions (Africa,

Table 2.5 Future climate projections for ARC3.2 Cities.¹²

	2020s	2050s	2080s
Temperature	+ 0.7 to 1.6°C	+ 1.4 to 3.1°C	+ 1.7 to 5.0°C
Precipitation	-7 to +10%	-9 to +14%	-11 to +20%
Sea Level Rise	+ 4 to 18 cm	14 to 56 cm	+ 21 to 118 cm

Asia and Australia, Europe, Latin America, and North America) ARC3.2 Cities include Case Study Docking Station cities, UCCRN Regional Hub cities, UCCRN project cities, and cities of ARC3.2 Chapter Authors.

Temperatures in the ARC3.2 cities around the world are projected to increase by 0.7–1.6°C by the 2020s, 1.4–3.1°C t the 2050s, and 1.7–5.0°C by the 2080s (see Table 2.5).

Following from the UCCRN analysis and the IPCC AR5 (IPCC, 2013), the greatest increases in temperature by the 2080s are projected for cities in North America and northern Europe, with upward of between 6 and 7°C of warming by the end of the century under the high emissions scenario (see Figure 2.3). Cities located in and around these regions include Calgary, Helsinki, Warsaw, and Moscow. Non-equatorial regions of Africa are also projected to have large temperature increases, including Johannesburg.

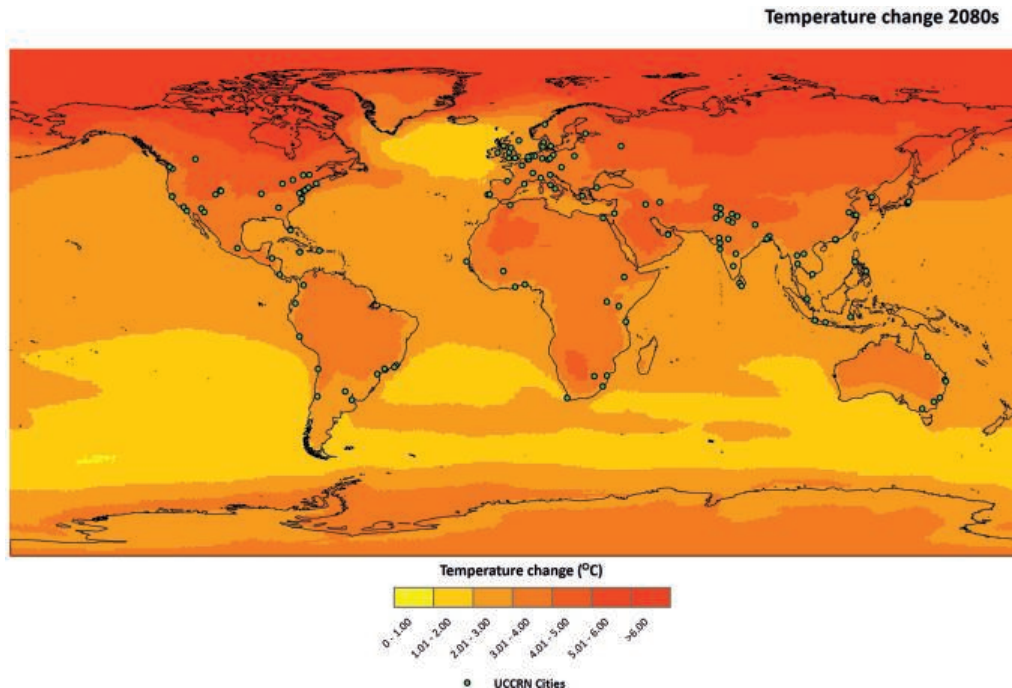


Figure 2.3 Projected temperature change in the 2080s. Temperature change projection is mean of 35 global climate models (GCMs) and two representative concentration pathways (RCP4.5 and RCP8.5). Colors represent the mean change in mean annual temperature (2070–2099 average relative to 1971–2000 average). Dots represent ARC3.2 cities. ARC3.2 Cities include Case Study Docking Station cities, UCCRN Regional Hub cities, UCCRN project cities, and cities of ARC3.2 Chapter Authors.

11 Because projected changes through time are generally similar between nearby gridboxes (Horton et al., 2011), a straightforward and easy-to-replicate single gridbox approach was used in this analysis.
 12 Projections for temperature and precipitation are based on 35GCMs and 2 RCPs. For each of the 153 ARC3.2 cities, the low estimate (10th percentile) and high estimate (90th percentile) were calculated. The range of values presented here is the average for each percentile averaged across all ARC3.2 cities. Projections are relative to the 1971–2000 base period.

Projections for sea level rise are based on a four-component approach that incorporates both local and global factors. For each of the 71 ARC3.2 coastal cities, the low estimate (10th percentile) and high estimate (90th percentile) were calculated. The range of values presented here is the average for each percentile averaged across all coastal ARC3.2 cities. The model-based components are from 24 GCMs and 2 RCPs. Projections are relative to the 2000–2004 base period.

ARC3.2 Cities include Case Study Docking Station cities, UCCRN Regional Hub cities, UCCRN project cities, and cities of ARC3.2 Chapter Authors.

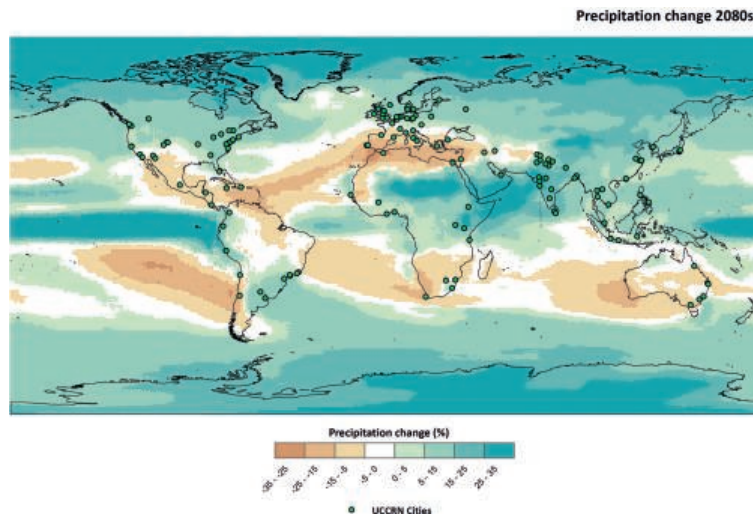


Figure 2.4 Projected precipitation change in the 2080s. Precipitation change projection is mean of 35 global climate models (GCMs) and two representative concentration pathways (RCP4.5 and RCP8.5). Colors represent the percentage change in mean annual precipitation (2070–2099 average relative to 1971–2000 average). Dots represent ARC3.2 cities. ARC3.2 Cities include Case Study Docking Station cities, UCCRN Regional Hub cities, UCCRN project cities, and cities of ARC3.2 Chapter Authors.

Similar rates of warming are projected for Asian cities such as Faisalabad, Tehran, and Delhi. Southern South America, South Asia, coastal Africa, and parts of Southeast Asia are also projected to see warming, however, at lower rates than these cities.

Precipitation in the ARC3.2 cities around the world is projected to change by -7 to $+10\%$ by the 2020s, -9 to $+14\%$ by the 2050s, and -11 to $+20\%$ by the 2080s (see Table 2.5). Projections for precipitation are characterized by greater uncertainty than those for temperature because GCMs have difficulty capturing the small-scale processes and climate variability that influence precipitation.

By the end of the century, increased precipitation is projected for near-equatorial areas in the Middle East, Africa, and portions of Asia including India and China (see Figure 2.4). Cities with projected precipitation increases include Bangalore, Colombo, and Dakar. Northern portions of North America and Europe are also projected to see increased precipitation.

Drier conditions are generally projected for northernmost Africa and southern Europe, including the cities of Rome, Naples, and Jerusalem. Some areas of Central and South America (Mexico City, Santiago, and Santo Domingo), Australia (Melbourne), and southern Africa (Cape Town) are also projected to see decreased precipitation by the end of the century under the high emissions scenario.

2.6.3 Sea Level Rise, Coastal Storms, and Flooding

Globally, many cities face faster local sea level rise than the global average due to subsidence caused by sediment compaction and groundwater withdrawal (Nicholls, 1995; Syvitski et al., 2009) (see Chapter 9, Coastal Zones). This is of significant

concern because many of the world's largest cities are located along the coast (Hanson et al., 2011). The processes of subsidence and groundwater withdrawal accelerate local sea level rise and thereby increase the vulnerability of urban areas. A study analyzing 40 river deltas globally, where Bangkok, Cairo, Cartagena, and Shanghai, are located, found that anthropogenic activities (changes in land-water storage and sediments) are the dominant contributors to observed sea level rise in many of these locations (Ericson et al., 2006). Rates of sea level rise in Manila and Bangkok exceed the global average, with the relative rise attributed to groundwater extraction and subsidence (Cazenave and Le Cozannet, 2014).

Projections for sea level rise are developed using both local and regional components based on GCMs and expert assessment of scientific literature (see Annex 2, Climate Projections for ARC3.2 Cities). For the ARC3.2 sea level rise projections, the following four components are used: 1) changes in ocean height (local); 2) thermal expansion (global); 3) loss of ice from glaciers, ice caps, and land-based ice sheets (global); and 4) land water storage (global).¹³ For each of these components of sea level rise, a set of distribution points are estimated and summed to give the total sea level rise projection (NPCC, 2015). These projections are expressed relative to the 2000–2004 baseline period. The timeslices are centered on a given decade. For example, the 2050s timeslice refers to the period from 2050 to 2059.

Sea level in 71 ARC3.2 coastal cities is projected to rise 4–18 centimeters by the 2020s; 14–56 centimeters by the 2050s, and 21–118 centimeters by the 2080s (see Table 2.5).¹⁴ Local effects, such as groundwater extraction, are not captured in the methods used for sea level rise projections here. However, they should be included in comprehensive city assessments if the data are available.

¹³ Two additional local components that can be incorporated into city-specific sea level rise projections are vertical land motions and the gravitational, rotational, and elastic "fingerprints" of ice loss. For most cities, the additional change in sea level rise projected from these components is approximately an order of magnitude smaller over the 21st-century timescale than the total projections. Exceptions may include (1) some delta cities such as Jakarta experiencing rapid sinking associated, for example, with groundwater withdrawal and (2) cities near any glacier or ice sheet that experiences rapid 21st-century mass loss.

¹⁴ For each of the coastal cities, the low estimate (10th percentile) and high estimate (90th percentile) were calculated. The range of values presented here are the average for each percentile averaged across all 52 cities.

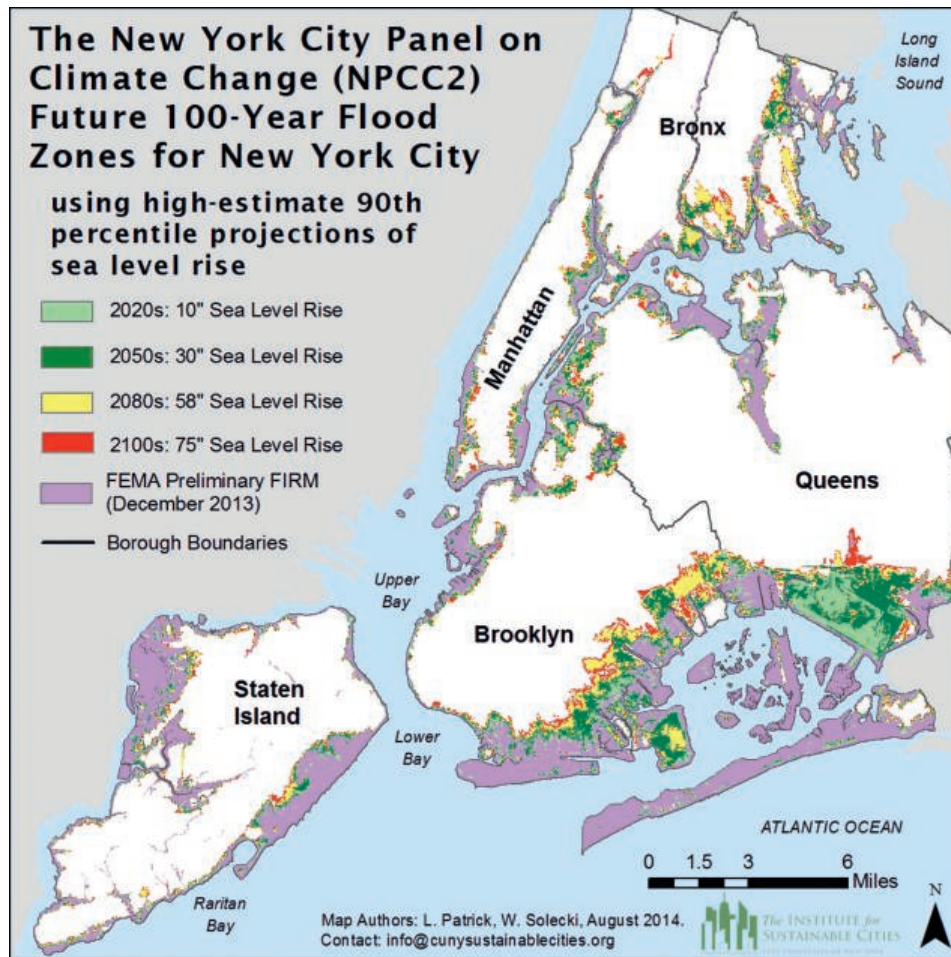


Figure 2.5 Potential areas that could be impacted by the 100-year flood in the 2020s, 2050s, 2080s, and 2100 based on projections of the high-estimate 90th percentile New York City Panel on Climate Change (NPCC2) sea level rise scenario. Map developed using the static approach. Note: This map is subject to limitations in accuracy as a result of the quantitative models, datasets, and methodology used in its development. The map and data should not be used to assess actual coastal hazards, insurance requirements, or property values or be used in lieu of flood insurance rate maps (FIRMS) issued by the Federal Emergency Management Agency (FEMA). The flood areas delineated in no way represent precise flood boundaries but rather illustrate three distinct areas of interest: (1) areas currently subject to the 100-year flood that will continue to be subject to flooding in the future, (2) areas that do not currently flood but are expected to potentially experience the 100-year flood in the future, and (3) areas that do not currently flood and are unlikely to do so in the timeline of the climate scenarios used by the NPCC (end of the current century).

Source: NPCC, 2015

Because sea level rise is not spatially uniform, cities will differ in how much sea level rise they will experience. For examples, some studies have found that the coastal Northeast United States, which includes large urban population centers such as New York, Boston, and Washington, D.C., have experienced, and may continue to experience, faster sea level rise than the global average due to a weakening of the Gulf Stream (Yin et al., 2009). Megacities are experiencing a triple threat of sea level rise associated with climate change, land sinking, and growing concentrations of people and assets near the coast (see Chapter 9, Coastal Zones).

In the future, the magnitude and frequency of coastal flooding may change due to changes in sea level and/or changes in coastal storms. Many coastal cities are not prepared for the coastal flood risks they face today, and the threat is exacerbated by sea level rise. A recent study found that cities in the United States saw more than 10-fold increases in nuisance flood events (floods that cause an inconvenience to the public, such as road closures or

clogged storm drains) over the past 60 years (Sweet and Park 2014). For these locations, coastal flooding now occurs at times of high tide and in minor coastal flood events due to observed changes in sea level and local land processes.

How coastal storms like tropical cyclones and mid-latitude storms may change in the future is still difficult to project (IPCC, 2013), although some studies suggest that as the upper oceans warm, the strongest tropical cyclones may tend to become stronger, and mid-latitude storms may tend to move closer to the poles (IPCC, 2012; IPCC, 2013; Colle et al., 2013). Although the implications of coastal storm changes for individual cities are highly uncertain, it is very certain that sea level rise will lead to large changes in coastal flood frequency. For example, in New York, by the 2080s, the current 100-year flood (a flood with a 1% annual chance of occurrence) is projected to become an approximately once-in-eight-year event (NPCC, 2015) (see Figure 2.5 and Table 2.6).

Table 2.6 Future flood recurrence intervals at the Battery, New York.
Source: NPCC, 2015

	Low estimate (10th percentile)	Middle range (25th–75th percentile)	High estimate (90th percentile)
2020s			
Annual chance of today's 100-year flood (1%)	1.1%	1.1–1.4%	1.5%
2050s			
Annual chance of today's 100-year flood (1%)	1.4%	1.6–2.4%	3.6%
2080s			
Annual chance of today's 100-year flood (1%)	1.7%	2.0–5.4%	12.7%

The change in coastal flood frequency associated with a given amount of sea level rise is highly dependent on the baseline distribution of coastal flooding (Tibaldi et al., 2012; Kopp et al., 2014). For cities like Lagos and San Francisco that do not experience large storm surges, even small amounts of sea level rise can lead to large increases in the frequency of coastal flooding (Strauss et al., 2012). In contrast, coastal regions that historically experience large storm surges (such as much of the northern Gulf of Mexico coast and parts of the coastline along the northwest Pacific Ocean) are projected to see smaller increases in coastal flood frequency associated with the sea level rise effect. When storms do occur, sea level rise means that the area inundated expands dramatically for low-lying and flat areas; this is less of a concern for coastal cities with steeper coastlines, such as Lima (Weiss et al., 2011).

Given the increased vulnerability that coastal cities have to sea level rise and coastal flooding, employment and improvement of mapping techniques such as geographic information system (GIS), global positioning system (GPS), and Light Detection and Ranging (LIDAR) could help urban areas plan for the future. For example, a comprehensive geodetic-based mapping survey of Jakarta found that land subsidence in the city is strongly linked to ground water extraction (Abidin, 2001). Identification of coastal risks through these technologies could identify vulnerable neighborhoods, and, therefore, where resources could be targeted in future flooding events.

2.6.4 Use of Climate Projections

Future climate projections from both GCMs and RCMs are being used by cities across the globe in a variety of applications (see Annexes 4 and 5; ARC3.2 Case Study Docking Station, www.uccrn.org/casestudies). Projections can be used to inform citywide adaptation plans, as has been done in New York (Rosenzweig and

Solecki, 2010), and London (LCCP, 2002). City sector-specific uses of climate projection examples include watershed modeling in Seoul (Chung et al., 2011), transportation planning in Stockholm (Gidhagen et al., 2012), and evaluating air pollution in Melbourne (Coutts et al., 2008). Outputs and projections from RCMs can be used to understand sector-specific climate impacts, such as how warming temperatures will impact public health in cities (Dessai, 2003; Bell et al., 2007; Knowlton et al., 2007; Casati et al., 2013).

Improving the process of the co-generation of climate risk information and interactions between scientists and stakeholders is under way (e.g., Lemos and Morehouse, 2005; Mauser et al., 2013), and these types of projections are already being used to inform adaptation strategies. Scientific expert panels have been formed in cities such as Quito, New York, and London for the purpose of providing the best available information for city governments to use in creating long-term municipal adaptation strategies to deal with the local impacts of climate change. Climate projections developed by these groups help to guide investments in flood management, infrastructure improvements, urban cooling techniques, and the development of emergency heat wave response plans (NPCC, 2015; Johnson and Breil, 2012; Zambrano-Barragán et al., 2011). Community involvement in the development of such climate actions plans is being solicited in cities like Quito and Durban. This information is being used to help implement building retrofit plans, form health network systems throughout the urban population, and improve emergency management during landslides and mudslides (Walsh et al., 2013; Johnson and Breil, 2012; eThekweni Municipality, 2011).

In places where infrastructure is not a viable option to prevent damage from extreme events, climate risk information is being used to identify vulnerable groups so that they can be moved out of harm's way. For example, in Ho Chi Minh City, stakeholder–scientist interactions that utilize flood impact models have led decision-makers to relocate low-income slum settlements out of the flood plain (Vietnam Climate Adaptation Partnership, 2013). These cases show that co-generated science is helping to prepare cities for the worst effects of climate change because the information is tailored to the needs of decision-makers at the local level, which is most relevant for city planning.

2.6.5 Advances in Urban Climate Science Research

In recent years, use of big data, new instruments, and falling costs of high-powered computing have enabled better understanding of extreme events and microclimatic variations within cities. Crowdsourcing, data mining (Muller et al., 2015), and the diffusion of small, inexpensive sensors that monitor climate-related variables are helping fill gaps in urban meteorological data that hinder understanding of these complex environments (Chen et al., 2012). Improved remote sensing technologies are being explored in Istanbul and Paris (Sismanidis et al., 2015), and Guangzhou (Guo et al., 2015). As these innovations emerge, they are also being used to facilitate the real-time monitoring of hazards, climate, and associated impacts such as air quality problems and health hazards in

coastal waterways. Developing advanced climate change indicators and monitoring systems, such as in New York (Solecki et al., 2015), and building on existing networks to integrate new instruments and indicators as in Birmingham, UK (Chapman et al., 2015), will become essential for research and adaptation in the future.

Urban climate models (from the building to full-city scale) have diversified and become more sophisticated in the past decade. Recent model comparison efforts have identified common characteristics of the best models and opportunities for improvement, such as better measurement of key parameters (Best and Grimmond, 2014) and integration with urban climate monitoring (Chen et al., 2012). Other research priorities in urban climate modeling include refining the estimation of heat fluxes between urban surfaces and the surrounding air; improving the simulation of anthropogenic heat inputs from traffic and buildings; and integrating dynamics, aerosol, and hydrology components to advance urban precipitation modeling (Chen et al., 2012). Downscaling of global and regional climate model projections for urban areas continues to advance with improved statistical techniques (Lauwaet et al., 2015), while the models themselves better simulate city-relevant processes such as the urban canopy and ocean–atmospheric interactions in coastal cities (Rummukainen et al., 2015) and are developed for use in impacts research (Mearns et al., 2015).

2.7 Conclusions and Recommendations

Cities are uniquely vulnerable to climate hazards, as well as being centers of greenhouse gas emissions. From a climate perspective, the urban heat island increases the frequency, duration, and intensity of heat waves beyond that associated with climate change; coastal cities are also sinking due to urban activities at the same time that sea levels are rising along the majority of the world’s coastlines. More research is needed on joint risks associated with climate change, such as (1) combined impacts of heat and humidity; (2) sequences of extreme events, such as a tropical cyclone followed by a heat wave; and (3) interactions between cold air outbreaks and poor air quality. Additionally and particularly for cities in developing countries, limited data availability and scientific capacity remain major challenges. More research is also needed on how climate information can inform the evaluation of adaptation and mitigation programs, particularly as these programs are being increasingly implemented in the world’s innovative cities.

Chapter 2 Urban Climate Science

References

- Abidin, H. Z., Djaja, R., Darmawan, D., Hadi, S., Akbar, A., Rajjiowiryono, H., Sudibyo, Y., Meilano, I., Kasuma, M. A., Kahar, J., and Subarya, C. (2001). Land subsidence of Jakarta (Indonesia) and its geodetic monitoring system *Natural Hazards* **23**(2–3), 365–387.
- Adamowski, J., and Prokoph, A. (2013). Assessing the impacts of the urban heat island effect on streamflow patterns in Ottawa, Canada. *Journal of Hydrology* **496**, 225–237.
- Alexander, L. V., Zhang, X., Peterson, T. C., Caesar, J., Gleason, B., Klein Tank, A. M. G., Haylock, M., Collins, D., Trewin, B., Rahimzadeh, F., Tagipour, A., Rupa Kumar, K., Revadekar, J., Griffiths, G., Vincent, L., Stephenson, D. B., Burn, J., Aguilar, E., Brunet, M., Taylor, M., New, M., Zhai, P., Rusticucci, M., and Vazquez-Aguirre, J. L. (2006). Global observed changes in daily climate extremes of temperature and precipitation. *Journal of Geophysical Research: Atmospheres* **111**(D5).
- Anniballe, R., Bonafoni, S., and Pichierri, M. (2014). Spatial and temporal trends of the surface and air heat island over Milan using MODIS data. *Remote Sensing of Environment* **150**(0), 163–171.
- Arnfield, A. J. (2003). Two decades of urban climate research: a review of turbulence, exchanges of energy and water, and the urban heat island. *International Journal of Climatology* **23**(1), 1–26.
- Balling, R. C., and Gober, P. (2007). Climate variability and residential water use in the city of Phoenix, Arizona. *Journal of Applied Meteorology and Climatology* **46**(7), 1130–1137.
- Basara, J. B., Illston, B. G., Fiebrich, C. A., Browder, P. D., Morgan, C. R., McCombs, A., Bostic, J. P., McPherson, R. A., Schroeder, A. J., and Crawford, K. C. (2011). The Oklahoma City microne. *Meteorological Applications* **18**(3), 252–261.
- Baxter, S., and Nigam, S. (2013). A subseasonal teleconnection analysis: PNA development and its relationship to the NAO. *Journal of Climate* **26**(18), 6733–6741.
- Bell, M. L., Goldberg, R., Hogrefe, C., Kinney, P. L., Knowlton, K., Lynn, B., Rosenthal, J., Rosenzweig, C., and Patz, J. A. (2007). Climate change, ambient ozone, and health in 50 US cities. *Climatic Change* **82**(1), 61–76.
- Bertaccini, P., Dukic, V., and Ignaccolo, R. (2012). Modeling the short-term effect of traffic and meteorology on air pollution in Turin with generalized additive models. *Advances in Meteorology* **2012**, 16.
- Best, M. J., and Grimmond, C. S. B. (2014). Key conclusions of the first International Urban Land Surface Model Comparison Project. *Bulletin of the American Meteorological Society* **96**(5), 805–819.
- Blake, R., Grimm, A., Ichinose, T., Horton, R., Gaffin, S., Jiong, S., Bader, D., and Cecil, D. W. (2011). Urban climate: Processes, trends, and projections. In Rosenzweig, C., Solecki, W. D., Hammer, S. A., and Mehrotra, S. (eds.), *Climate Change and Cities: First Assessment Report of the Urban Climate Change Research Network* (43–81). Cambridge University Press.
- Bond, N. A., and Vecchi, G. A. (2003). The influence of the Madden–Julian Oscillation on precipitation in Oregon and Washington. *Weather and Forecasting* **18**(4), 600–613.
- Bornstein, R., and Lin, Q. (2000). Urban heat islands and summertime convective thunderstorms in Atlanta: three case studies. *Atmospheric Environment* **34**(3), 507–516.
- Bouma, M., and Dye, C. (1997). Cycles of malaria associated with El Niño in Venezuela. *Journal of the American Medical Association* **278**(21), 1772–1774.
- Burian, S. J., and Shepherd, J. M. (2005). Effect of urbanization on the diurnal rainfall pattern in Houston. *Hydrological Processes* **19**(5), 1089–1103.
- Cai, W., Borlace, S., Lengaigne, M., van Rensch, P., Collins, M., Vecchi, G., Timmermann, A., Santos, A., McPhaden, M. J., Wu, L., England, M. H., Wang, G., Guilyardi, E., and Jin, F. -F. (2014). Increasing frequency of extreme El Niño events due to greenhouse warming. *Nature Climate Change* **4**(2), 111–116.
- Casati, B., Yagouti, A., and Chaumont, D. (2013). Regional climate projections of extreme heat events in nine pilot Canadian communities for public health planning. *Journal of Applied Meteorology and Climatology* **52**(12), 2669–2698.
- Cazenave, A., and Cozannet, G. L. (2014). Sea level rise and its coastal impacts. *Earth’s Future* **2**(2), 15–34.

- Chang, B., Wang, H. -Y., Peng, T. -Y., and Hsu, Y. -S. (2010). Development and evaluation of a city-wide wireless weather sensor network. *Journal of Educational Technology & Society* **13**(3), 270–280.
- Chang, H., Praskievicz, S., and Parandvash, H. (2014). Sensitivity of urban water consumption to weather and climate variability at multiple temporal scales: The case of Portland, Oregon *International Journal of Geospatial and Environmental Research* **1**(1).
- Chapman, L., Muller, C. L., Young, D. T., Warren, E. L., Grimmond, C. S. B., Cai, X. -M., and Ferranti, E. J. S. (2015). The Birmingham Urban Climate Laboratory: An open meteorological test bed and challenges of the smart city. *Bulletin of the American Meteorological Society* **96**(9), 1545–1560.
- Chen, F., Bornstein, R., Grimmond, S., Li, J., Liang, X., Martilli, A., Miao, S., Voogt, J., and Wang, Y. (2012). Research priorities in observing and modeling urban weather and climate. *Bulletin of the American Meteorological Society* **93**(11), 1725–1728.
- Chen, F., Yang, X., and Zhu, W. (2014). WRF simulations of urban heat island under hot-weather synoptic conditions: The case study of Hangzhou City, China *Atmospheric Research* **138** (2014), 364–377.
- Cherry, J., Cullen, H., Visbeck, M., Small, A., and Uvo, C. (2005). Impacts of the North Atlantic Oscillation on Scandinavian hydropower production and energy markets. *Water Resources Management* **19**(6), 673–691.
- Cheval, S., and Dumitrescu, A. (2009). The July urban heat island of Bucharest as derived from modis images. *Theoretical and Applied Climatology* **96**(1–2), 145–153.
- Childs, P., and Raman, S. (2005). Observations and numerical simulations of urban heat island and sea breeze circulations over New York City. *Pure and Applied Geophysics* **162**(10), 1955–1980.
- Christensen, J. H., Krishna Kumar, K., Aldrian, E., An, S. -I., Cavalcanti, I. F. A., Castro, M. D., Dong, W., Goswami, P., Hall, A., Kanyanga, J. K., Kitoh, A., Kossin, J., Lau, N. -C., Renwick, J., Stephenson, D. B., Xie, S. -P., and Zhou, T. (2013). Climate phenomena and their relevance for future regional climate change. In Stocker, T. F., Qin, D., Plattner, G. -K., Tignor, M., Allen, S. K., Boschung, J., Nauels, A., Xia, Y., Bex, V., and Midgley, P. M. (eds.), *Climate Change 2013: The Physical Science Basis. Contribution of Working Group I to the Fifth Assessment Report of the Intergovernmental Panel on Climate Change* (1217–1308). Cambridge University Press.
- Chung, E. -S., Park, K., and Lee, K. S. (2011). The relative impacts of climate change and urbanization on the hydrological response of a Korean urban watershed. *Hydrological Processes* **25**(4), 544–560.
- City of New York. (2013). *New York City Special Initiative on Rebuilding and Resiliency: A Stronger, More Resilient New York*. City of New York.
- Colle, B. A., Zhang, Z., Lombardo, K. A., Chang, E., Liu, P., and Zhang, M. (2013). Historical evaluation and future prediction of eastern North American and western Atlantic extratropical cyclones in the CMIP5 models during the cool season. *Journal of Climate* **26**(18), 6882–6903.
- Collins, M. (2005). El Niño- or La Niña-like climate change?. *Climate Dynamics* **24**(1), 89–104.
- Collins, M., An, S. -I., Cai, W., Ganachaud, A., Guilyardi, E., Jin, F. -F., Jochem, M., Lengaigne, M., Power, S., Timmermann, A., Vecchi, G., and Wittenberg, A. (2010). The impact of global warming on the tropical Pacific Ocean and El Niño. *Nature Geoscience* **3**(6), 391–397.
- Connors, J., Galletti, C., and Chow, W. L. (2013). Landscape configuration and urban heat island effects: Assessing the relationship between landscape characteristics and land surface temperature in Phoenix, Arizona *Landscape Ecology* **28**(2), 271–283.
- Cooper, M. J., Martin, R. V., van Donkelaar, A., Lamsal, L., Brauer, M., and Brook, J. R. (2012). A satellite-based multi-pollutant index of global air quality *Environmental Science & Technology* **46**(16), 8523–8524.
- Coutts, A. M., Beringer, J., and Tapper, N. J. (2008). Investigating the climatic impact of urban planning strategies through the use of regional climate modelling: A case study for Melbourne, Australia. *International Journal of Climatology* **28**(14), 1943–1957.
- Cramer, W., Yohe, G. W., Auffhammer, M., Huggel, C., Molau, U., Dias, M. A. F. S., Solow, A., Stone, D. A., and Tibig, L. (2014). Detection and attribution of observed impacts. In Field, C. B., Barros, V. R., Dokken, D. J., Mach, K. J., Mastrandrea, M. D., Bilir, T. E., Chatterjee, M., Ebi, K. L., Estrada, Y. O., Genova, R. C., Girma, B., Kissel, E. S., Levy, A. N., MacCracken, S., Mastrandrea, P. R., and White, L. L. (eds.), *Climate Change 2014: Impacts, Adaptation, and Vulnerability. Part A: Global and Sectoral Aspects. Contribution of Working Group II to the Fifth Assessment Report of the Intergovernmental Panel of Climate Change* (979–1037). Cambridge University Press.
- Currie, B. A., and Bass, B. (2008). Estimates of air pollution mitigation with green plants and green roofs using the UFORE model. *Urban Ecosystems* **11**(4), 409–422.
- Dabberdt, W., Koistinen, J., Poutiainen, J., Saltikoff, E., and Turtiainen, H. (2005). Research: The Helsinki Mesoscale Testbed: An invitation to use a new 3-D observation network *Bulletin of the American Meteorological Society* **86**(7), 906–907.
- Davini, P., and Cagnazzo, C. (2014). On the misinterpretation of the North Atlantic Oscillation in CMIP5 models. *Climate Dynamics* **43**(5), 1497–1511.
- Dawson, J. P., Bryan, J. B., Darrell, A. W., and Christopher, P. W. (2014). Understanding the meteorological drivers of US particulate matter concentrations in a changing climate. *Bulletin of the American Meteorological Society* **95**(4), 521–532.
- Deser, C., Knutti, R., Solomon, S., and Phillips, A. S. (2012). Communication of the role of natural variability in future North American climate. *Nature Climate Change* **2**(11), 775–779.
- Dessai, S. (2003). Heat stress and mortality in Lisbon Part II. An assessment of the potential impacts of climate change. *International Journal of Biometeorology* **48**(1), 37–44.
- Dobre, A., Arnold, S. J., Smalley, R. J., Boddy, J. W. D., Barlow, J. F., Tomlin, A. S., and Belcher, S. E. (2005). Flow field measurements in the proximity of an urban intersection in London, UK. *Atmospheric Environment* **39**(26), 4647–4657.
- Dobrovolný, P. (2013). The surface urban heat island in the city of Brno (Czech Republic) derived from land surface temperatures and selected reasons for its spatial variability. *Theoretical and Applied Climatology* **112**(1–2), 89–98.
- Earnest, A., Tan, S. B., and Wilder-Smith, A. (2012). Meteorological factors and El Niño southern oscillation are independently associated with dengue infections. *Epidemiology & Infection* **140**(07), 1244–1251.
- Emmanuel, R., and Krüger, E. (2012). Urban heat island and its impact on climate change resilience in a shrinking city: The case of Glasgow, UK. *Building and Environment* **53**(0), 137–149.
- Ericson, J. P., Vörösmarty, C. J., Dingman, S. L., Ward, L. G., and Meybeck, M. (2006). Effective sea-level rise and deltas: Causes of change and human dimension implications. *Global and Planetary Change* **50**(1–2), 63–82.
- eThekwin Municipality. (2011). *Durbans Municipal Climate Protection Programme: Climate Change Adaptation Planning for a Resilient City* (36). Durban, South Africa, eThekwin Municipality Environmental Planning and Climate Protection Department.
- Formiga-Johnsson, R., and Britto, A. (2009). *Climate Variability And Competing Demands For Urban Water Supply: Reducing Vulnerability Through River Basin Governance In Brazil*. Marseille: Fifth Urban Research Symposium 2009.
- Gaffin, S. R., Rosenzweig, C., Khanbilvardi, R., Parshall, L., Mahani, S., Glickman, H., Goldberg, R., Blake, R., Slosberg, R. B., and Hillel, D. (2008). Variations in New York City's urban heat island strength over time and space *Theoretical and Applied Climatology* **94**(1–2), 1–11.
- Gedzelman, S. D., Austin, S., Cermak, R., Stefano, N., Partridge, S., Quesenberry, S., and Robinson, D. A. (2003). Mesoscale aspects of the urban heat island around New York City. *Theoretical and Applied Climatology* **75**(1–2), 29–42.
- Giannaros, T. M., and Melas, D. (2012). Study of the urban heat island in a coastal Mediterranean city: The case study of Thessaloniki, Greece. *Atmospheric Research* **118**(0), 103–120.

- Gidhagen, L., Engardt, M., Lövenheim, B., and Johansson, C. (2012). Modeling effects of climate change on air quality and population exposure in urban planning scenarios. *Advances in Meteorology* **2012**, 12.
- Goldbach, A., and Kuttler, W. (2013). Quantification of turbulent heat fluxes for adaptation strategies within urban planning. *International Journal of Climatology* **33**(1), 143–159.
- Gramsch, E., Cereceda-Balic, F., Oyola, P., and von Baer, D. (2006). Examination of pollution trends in Santiago de Chile with cluster analysis of PM10 and Ozone data. *Atmospheric Environment* **40**(28), 5464–5475.
- Grimm, A. M., and Tedeschi, R. G. (2009). ENSO and Extreme Rainfall Events in South America. *Journal of Climate* **22**(7), 1589–1609.
- Guo, G., Wu, Z., Xiao, R., Chen, Y., Liu, X., and Zhang, X. (2015). Impacts of urban biophysical composition on land surface temperature in urban heat island clusters. *Landscapes and Urban Planning* **135**, 1–10.
- Gurjar, B. R., Butler, T. M., Lawrence, M. G., and Lelieveld, J. (2008). Evaluation of emissions and air quality in megacities. *Atmospheric Environment* **42**(7), 1593–1606.
- Han, J. -Y., Baik, J. -J., and Lee, H. (2014). Urban impacts on precipitation. *Asia-Pacific Journal of Atmospheric Sciences* **50**(1), 17–30.
- Hansen, J., Ruedy, R., Sato, M., Imhoff, M., Lawrence, W., Easterling, D., Peterson, T., and Karl, T. (2001). A closer look at United States and global surface temperature change. *Journal of Geophysical Research: Atmospheres* **106**(D20), 23947–23963.
- Hansen, J., Ruedy, R., Sato, M., and Lo, K. (2010). Global surface temperature change. *Reviews of Geophysics* **48**(4), RG4004.
- Hanson, S., Nicholls, R., Ranger, N., Hallegatte, S., Corfee-Morlot, J., Herweijer, C., and Chateau, J. (2011). A global ranking of port cities with high exposure to climate extremes. *Climatic Change* **104**(1), 89–111.
- Hausfather, Z., Menne, M. J., Williams, C. N., Masters, T., Broberg, R., and Jones, D. (2013). Quantifying the effect of urbanization on US Historical Climatology Network temperature records. *Journal of Geophysical Research: Atmospheres* **118**(2), 481–494.
- Hay, C. C., Morrow, E., Kopp, R. E., and Mitrovica, J. X. (2015). Probabilistic reanalysis of twentieth-century sea-level rise. *Nature* **517**(7535), 481–484.
- Hicks, B. B., Callahan, W. J., Pendergrass, W. R., Dobosy, R. J., and Novakovskaia, E. (2012). Urban turbulence in space and in time. *Journal of Applied Meteorology and Climatology* **51**(2), 205–218.
- Hiroynuki, K., Nawata, K., Suzuki-Parker, A., Takane, Y., and Furuhashi, N. (2013). Mechanism of precipitation increase with urbanization in Tokyo as revealed by ensemble climate simulations. *Journal of Applied Meteorology and Climatology* **53**(4), 824–839.
- Hoerling, M., Eischeid, J., and Perlwitz, J. (2010). Regional precipitation trends: Distinguishing natural variability from anthropogenic forcing. *Journal of Climate* **23**(8), 2131–2145.
- Holmer, B., and Eliasson, I. (1999). Urban–rural vapour pressure differences and their role in the development of urban heat islands. *International Journal of Climatology* **19**(9), 989–1009.
- Horton, R. M., Gornitz, V., Bader, D. A., Ruane, A. C., Goldberg, R., and Rosenzweig, C. (2011). Climate hazard assessment for stakeholder adaptation planning in New York City. *Journal of Applied Meteorology and Climatology* **50**(11), 2247–2266.
- Hung, T., D. Uchihama, S. Oci, and Y. Yasuoka (2006). Assessment with satellite data of the urban heat island effects in Asian mega cities. *International Journal of Applied Earth Observation and Geoinformation* **8**, 34–48.
- Hung, T. K., and Wo, O. C. (2012). Development of a Community Weather Information Network (Co-WIN) in Hong Kong. *Weather* **67**(2), 48–50.
- Hurrell, J. W., Kushnir, Y., Ottensm, G., and Visbeck, M. (2003). An overview of the North Atlantic oscillation. *Geophysical Monograph-American Geophysical Union* **134**, 1–36.
- Imhoff, M. L., Zhang, P., Wolfe, R. E., and Bounoua, L. (2010). Remote sensing of the urban heat island effect across biomes in the continental USA. *Remote Sensing of Environment* **114**(3), 504–513.
- Intergovernmental Panel on Climate Change (IPCC). (2013). *Climate Change 2013: The Physical Science Basis. Contribution of Working Group I to the Fifth Assessment Report of the Intergovernmental Panel on Climate Change*. Cambridge University Press.
- Intergovernmental Panel on Climate Change (IPCC). (2012). *Managing the Risks of Extreme Events and Disasters to Advance Climate Change Adaptation. A Special Report of Working Groups I and II of the Intergovernmental Panel on Climate Change*. C. B. Field, V. R. Barros, T. F. Stocker et al. (eds.). Cambridge University Press. 582.
- Jacob, D. J., and Winner, D. A. (2009). Effect of climate change on air quality. *Atmospheric Environment* **43**(1), 51–63.
- Janhäll, S., Olofson, K. F. G., Andersson, P. U., Pettersson, J. B. C., and Hallquist, M. (2006). Evolution of the urban aerosol during winter temperature inversion episodes. *Atmospheric Environment* **40**(28), 5355–5366.
- Jauregui, E. (1997). Heat island development in Mexico City. *Atmospheric Environment* **31**(22), 3821–3831.
- Jauregui, E., and Romales, E. (1996). Urban effects on convective precipitation in Mexico city. *Atmospheric Environment* **30**(20), 3383–3389.
- Jiong, S. (2004). Shanghai’s land use pattern, temperature, relative humidity, and precipitation. *Atlas of Shanghai Urban Geography*.
- Johnson, K., and Breil, M. (2012). Conceptualizing urban adaptation to climate change: Findings from an applied adaptation assessment. In Carraro, C. (ed.), *Climate Change and Sustainable Development Series* (66), Venice, Italy, CMCC Research Paper.
- Jones, P. D., Lister, D. H., and Li, Q. (2008). Urbanization effects in large-scale temperature records, with an emphasis on China. *Journal of Geophysical Research: Atmospheres* **113**(D16).
- Kalnay, E., and Cai, M. (2003). Impact of urbanization and land-use change on climate. *Nature* **423**(6939), 528–531.
- Karagulian, F., Belis, C. A., Dora, C. F. C., Prüss-Ustün, A. M., Bonjour, S., Adair-Rohani, H., and Amann, M. (2015). Contributions to cities’ ambient particulate matter (PM): A systematic review of local source contributions at global level. *Atmospheric Environment* **120**, 475–483.
- Katragkou, E., Zanis, P., Kioutsioukis, I., Tegoulas, I., Melas, D., Krüger, B. C., and Coppola, E. (2011). Future climate change impacts on summer surface ozone from regional climate-air quality simulations over Europe. *Journal of Geophysical Research: Atmospheres* **116**(D22).
- Katsoulis, B. D., and Theoharatos, G. A. (1985). Indications of the urban heat island in Athens, Greece. *Journal of Climate and Applied Meteorology* **24**(12), 1296–1302.
- Kerr, R. A. (2011). Time to adapt to a warming world, but where’s the science?. *Science* **334**(6059), 1052–1053.
- Kim, J. -S., Zhou, W., Cheung, H., and Chow, C. (2013). Variability and risk analysis of Hong Kong air quality based on Monsoon and El Niño conditions. *Advances in Atmospheric Sciences* **30**(2), 280–290.
- Klok, L., Zwart, S., Verhagen, H., and Mauri, E. (2012). The surface heat island of Rotterdam and its relationship with urban surface characteristics. *Resources, Conservation and Recycling* **64**, 23–29.
- Knowlton, K., Lynn, B., Goldberg, R. A., Rosenzweig, C., Hogrefe, C., Rosenthal, J. K., and Kinney, P. L. (2007). Projecting heat-related mortality impacts under a changing climate in the New York City region. *American Journal of Public Health* **97**(11), 2028–2034.
- Kopp, R. E., Horton, R. M., Little, C. M., Mitrovica, J. X., Oppenheimer, M., Rasmussen, D. J., Strauss, B. H., and Tebaldi, C. (2014). Probabilistic 21st and 22nd century sea-level projections at a global network of tide-gauge sites. *Earth’s Future* **2**(8), 383–406.
- Koskinen, J. T., Poutiainen, J., Schultz, D. M., Joffre, S., Koistinen, J., Saltikoff, E., Gregow, E., Turtiainen, H., Dabberdt, W. F., Damski, J., Eresmaa, N., Göke, S., Hyvärinen, O., Järvi, L., Karppinen, A., Kotro, J., Kuitunen, T., Kukkonen, J., Kulmala, M., Moisseev, D., Nurmi, P., Pohjola, H., Pylkkö, P., Vesala, T., and Viisanen, Y. (2010). The Helsinki testbed: A mesoscale measurement, research, and service platform. *Bulletin of the American Meteorological Society* **92**(3), 325–342.
- Kura, B., Verma, S., Ajdari, E., and Iyer, A. (2013). Growing public health concerns from poor urban air quality: Strategies for sustainable urban living. *Computational Water, Energy, and Environmental Engineering* **2**(02), 1.
- Kuttler, W., Weber, S., Schonnefeld, J., and Hesselschwerdt, A. (2007). Urban/rural atmospheric water vapour pressure differences and urban moisture excess in Krefeld, Germany. *International Journal of Climatology* **27**(14), 2005–2015.

- Lamsal, L. N., Martin, R. V., Parrish, D. D., and Krotkov, N. A. (2013). Scaling relationship for NO₂ pollution and urban population size: A satellite perspective. *Environmental Science & Technology* **47**(14), 7855–7861.
- Lauwaet, D., Hooyberghs, H., Maiheu, B., Lefebvre, W., Driesen, G., Van Looy, S., and De Ridder, K. (2015). Detailed urban heat island projections for cities worldwide: Dynamical downscaling CMIP5 global climate models. *Climate* **3**(2), 391.
- Lee, D. O. (1979). The influence of atmospheric stability and the urban heat island on urban-rural wind speed differences. *Atmospheric Environment* (1967) **13**(8), 1175–1180.
- Lemonsu, A., and Masson, V. (2002). Simulation of a summer urban breeze over Paris. *Boundary-Layer Meteorology* **104**(3), 463–490.
- Lemos, M. C., Agrawal, A., Eakin, H., Nelson, D. R., Engle, N. L., and Johns, O. (2013). Building adaptive capacity to climate change in less developed countries. In Asrar, G. R., and Hurrell, J. W. (eds.), *Climate Science for Serving Society* (437–457). Springer Netherlands.
- Lemos, M. C., and Morehouse, B. J. (2005). The co-production of science and policy in integrated climate assessments. *Global Environmental Change* **15**(1), 57–68.
- Li, D., and Bou-Zeid, E. (2013). Synergistic interactions between urban heat islands and heat waves: The impact in cities is larger than the sum of its parts. *Journal of Applied Meteorology and Climatology* **52**(9), 2051–2064.
- Li, D., Bou-Zeid, E., Baeck, M. L., Jessup, S., and Smith, J. A. (2013). Modeling land surface processes and heavy rainfall in urban environments: Sensitivity to urban surface representations. *Journal of Hydrometeorology* **14**(4), 1098–1118.
- Lin, C. -Y., Chen, W. -C., Chang, P. -L., and Sheng, Y. -F. (2010). Impact of the urban heat island effect on precipitation over a complex geographic environment in northern Taiwan. *Journal of Applied Meteorology and Climatology* **50**(2), 339–353.
- London Climate Change Partnership (LCCP). (2002). *London's Warming. The Impacts of Climate Change on London: Technical Report* (311). LCCP.
- Luković, J., Blagojević, D., Kilibarda, M., and Bajat, B. (2015). Spatial pattern of North Atlantic oscillation impact on rainfall in Serbia. *Spatial Statistics* **14**(Part A), 39–52.
- Mackey, C. W., Lee, X., and Smith, R. B. (2012). Remotely sensing the cooling effects of city scale efforts to reduce urban heat island. *Building and Environment* **49**(0), 348–358.
- Major, D. C., and O'Grady, M. (2010). Adaptation Assessment Guidebook. In Rosenzweig, C., and Solecki, W. (eds.), *Climate Change Adaptation in New York City: Building a Risk Management Response* (229–292). Blackwell Publishing on behalf of the New York Academy of Sciences.
- Mantua, N. J., Hare, S., Zhang, Y., Wallace, J. M., and Francis, R. C. (1997). A Pacific interdecadal climate oscillation with impacts on salmon production. *Bulletin of the American Meteorological Society* **78**(6), 1069–1079.
- Marengo, A. J. (2004). Interdecadal variability and trends of rainfall across the Amazon basin. *Theoretical and Applied Climatology* **78**(1), 79–96.
- Mausser, W., Klepper, G., Rice, M., Schmalzbauer, B. S., Hackmann, H., Leemans, R., and Moore, H. (2013). Transdisciplinary global change research: The co-creation of knowledge for sustainability. *Current Opinion in Environmental Sustainability* **5**(3–4), 420–431.
- Mearns, L. O., Lettenmaier, D. P., and McGinnis, S. (2015). Uses of results of regional climate model experiments for impacts and adaptation studies: The example of NARCCAP. *Current Climate Change Reports* **1**(1), 1–9.
- Mikami, T., Ando, H., Morishima, W., Izumi, T., and Shioda, T. (2003). A new urban heat island monitoring system in Tokyo. In *Fifth International Conference on Urban Climate*, Lodz, Poland.
- Milly, P. C. D., Betancourt, J., Falkenmark, M., Hirsch, R. M., Kundzewicz, Z. W., Lettenmaier, D. P., and Stouffer, R. J. (2008). Stationarity is dead: Whither water management? *Science* **319**(5863), 573–574.
- Mishra, V., Ganguly, A. R., Nijssen, B., and Lettenmaier, D. P. (2015). Changes in observed climate extremes in global urban areas. *Environmental Research Letters* **10**(2), 024005.
- Mishra, V., and Lettenmaier, D. P. (2011). Climatic trends in major US urban areas, 1950–2009. *Geophysical Research Letters* **38**(16).
- Mohan, M., Y. Kikegawa, B. R. Gurjar, S. Bhati, A. Kandya, and K. Ogawa (2009). Assessment of Urban Heat Island Intensities over Delhi. *The Seventh International Conference on Urban Climate*. Yokohama, Japan.
- Morris, C. J. G., and Simmonds, I. (2000). Associations between varying magnitudes of the urban heat island and the synoptic climatology in Melbourne, Australia. *International Journal of Climatology* **20**(15), 1931–1954.
- Morris, C. J. G., Simmonds, I., and Plummer, N. (2001). Quantification of the influences of wind and cloud on the nocturnal urban heat island of a large city. *Journal of Applied Meteorology* **40**(2), 169–182.
- Moss, R. H., Edmonds, J. A., Hibbard, K. A., Manning, M. R., Rose, S. K., van Vuuren, D. P., Carter, T. R., Emori, S., Kainuma, M., Kram, T., Meehl, G. A., Mitchell, J. F. B., Nakicenovic, N., Riahi, K., Smith, S. J., Stouffer, R. J., Thomson, A. M., Weyant, J. P., and Wilbanks, T. J. (2010). The next generation of scenarios for climate change research and assessment. *Nature* **463**(7282), 747–756.
- Moss, R. H., Meehl, G. A., Lemos, M. C., Smith, J. B., Arnold, J. R., Arnot, J. C., Behar, D., Brasseur, G. P., Broomell, S. B., Busalacchi, A. J., Dessai, S., Ebi, K. L., Edmonds, J. A., Furlow, J., Goddard, L., Hartmann, H. C., Hurrell, J. W., Katzenberger, J. W., Liverman, D. M., Mote, P. W., Moser, S. C., Kumar, A., Pulwarty, R. S., Seyller, E. A., Turner, B. L., Washington, W. M., and Wilbanks, T. J. (2013). Hell and high water: Practice-relevant adaptation science. *Science* **342**(6159), 696–698.
- Muller, C. L., Chapman, L., Grimmond, C. S. B., Young, D. T., and Cai, X. (2013a). Sensors and the city: A review of urban meteorological networks. *International Journal of Climatology* **33**(7), 1585–1600.
- Muller, C. L., Chapman, L., Grimmond, C. S. B., Young, D. T., and Cai, X. (2013b). Toward a standardized metadata protocol for urban meteorological networks. *Bulletin of the American Meteorological Society* **94**(8), 1161–1185.
- Muller, C. L., Chapman, L., Johnston, S., Kidd, C., Illingworth, S., Foody, G., Overeem, A., and Leigh, R. R. (2015). Crowdsourcing for climate and atmospheric sciences: current status and future potential. *International Journal of Climatology* **35**(11), 3185–3203.
- Müller, N., Kuttler, W., and Barlag, A. -B. (2013). Counteracting urban climate change: adaptation measures and their effect on thermal comfort. *Theoretical and Applied Climatology* **115**(1), 243–257.
- New York City Panel on Climate Change (NPCC). (2015). *Building the Knowledge Base for Climate Resiliency: New York City Panel on Climate Change 2015 Report*. Annals of the New York Academy of Sciences.
- Nicholls, R. (1995). Coastal megacities and climate change. *GeoJournal* **37**(3), 369–379.
- Ning, L., and Bradley, R. S. (2015). Winter climate extremes over the northeastern United States and Southeastern Canada and teleconnections with large-scale modes of climate variability. *Journal of Climate* **28**(6), 2475–2493.
- Niyogi, D., Pyle, P., Lei, M., Arya, S. P., Kishitawal, C. M., Shepherd, M., Chen, F., and Wolfe, B. (2010). Urban modification of thunderstorms: An observational storm climatology and model case study for the Indianapolis urban region. *Journal of Applied Meteorology and Climatology* **50**(5), 1129–1144.
- Ohashi, Y., Genchi, Y., Kondo, H., Kikegawa, Y., Yoshikado, H., and Hirano, Y. (2007). Influence of air-conditioning waste heat on air temperature in Tokyo during summer: Numerical experiments using an urban canopy model coupled with a building energy model. *Journal of Applied Meteorology and Climatology* **46**(1), 66–81.
- Oke, T. R. (1978). *Boundary Layer Climate*. Routledge.
- Oke, T. R. (2006). Towards better scientific communication in urban climate. *Theoretical and Applied Climatology* **84**(1–3), 179–190.
- Overeem, A., Leijne, H., and Uijlenhoet, R. (2013). Country-wide rainfall maps from cellular communication networks. *Proceedings of the National Academy of Sciences* **110**(8), 2741–2745.
- Parker, D. E. (2006). A demonstration that large-scale warming is not urban. *Journal of Climate* **19**(12), 2882–2895.

- Patt, A., and Gwata, C. (2002). Effective seasonal climate forecast applications: Examining constraints for subsistence farmers in Zimbabwe. *Global Environmental Change* **12**(3), 185–195.
- Peterson, T. C. (2003). Assessment of urban versus rural *in situ* surface temperatures in the contiguous United States: No difference found. *Journal of Climate* **16**(18), 2941–2959.
- Power, S., Delage, F., Chung, C., Kociuba, G., and Keay, K. (2013). Robust twenty-first-century projections of El Niño and related precipitation variability. *Nature* **502**(7472), 541–545.
- Pozo-Vázquez, D., Esteban-Parra, J. M., Rodrigo, S. F., and Castro-Diez, Y. (2001). A study of NAO variability and its possible non-linear influences on European surface temperature. *Climate Dynamics* **17**(9), 701–715.
- Pugh, T. A. M., MacKenzie, A. R., Whyatt, J. D., and Hewitt, C. N. (2012). Effectiveness of green infrastructure for improvement of air quality in urban street canyons. *Environmental Science & Technology* **46**(14), 7692–7699.
- Rasmusson, E. M., and Wallace, J. M. (1983). Meteorological aspects of the El Niño/Southern Oscillation. *Science* **222**(4629), 1195–1202.
- Richards, K. (2005). Urban and rural dewfall, surface moisture, and associated canopy-level air temperature and humidity measurements for Vancouver, Canada. *Boundary-Layer Meteorology* **114**(1), 143–163.
- Rinner, C., and Hussain, M. (2011). Toronto’s urban heat island—Exploring the relationship between land use and surface temperature *Remote Sensing* **3**(6), 1251–1265.
- Robaa, S. M. (2003). Urban-suburban/rural differences over greater Cairo, Egypt. *Atmosfera* **16**(3), 157–171.
- Rosenzweig, C. and Solecki, W. (eds.). (2010). Climate change adaptation in New York City: Building a risk management response. New York City Panel on Climate Change 2010 Report. *Annals of the New York Academy of Sciences* 1196, 354.
- Rosenzweig, C., Solecki, W. D., Cox, J., Hodges, S., Parshall, L., Lynn, B., Goldberg, R., Gaffin, S., Slosberg, R. B., Savio, P., Watson, M., and Dunstan, F. (2009). Mitigating New York City’s heat island: Integrating stakeholder perspectives and scientific evaluation. *Bulletin of the American Meteorological Society* **90**(9), 1297–1312.
- Rotem-Mindali, O., Michael, Y., Helman, D., and Lensky, I. M. (2015). The role of local land-use on the urban heat island effect of Tel Aviv as assessed from satellite remote sensing. *Applied Geography* **56**(0), 145–153.
- Rummukainen, M., Rockel, B., Bärring, L., Christensen, J. H., and Reckermann, M. (2015). Twenty-first-century challenges in regional climate modeling. *Bulletin of the American Meteorological Society* **96**(8), ES135–ES138.
- Ryu, Y. -H., and Baik, J. -J. (2012). Quantitative analysis of factors contributing to urban heat island intensity. *Journal of Applied Meteorology and Climatology* **51**(5), 842–854.
- Seifert, A., Köhler, C., and Beheng, K. D. (2012). Aerosol-cloud-precipitation effects over Germany as simulated by a convective-scale numerical weather prediction model. *Atmospheric Chemistry and Physics* **12**(2), 709–725. doi: 10.5194/acp-12-709-2012
- Seiki, A., Nagura, M., Hasegawa, T., and Yoneyama, K. (2015). Seasonal onset of the Madden-Julian Oscillation and its relation to the south-eastern Indian Ocean cooling. *Journal of the Meteorological Society of Japan. Ser. II* **93A**, 139–156.
- Shepherd, J. M. (2006). Evidence of urban-induced precipitation variability in arid climate regimes. *Journal of Arid Environments* **67**(4), 607–628.
- Shepherd, J. M., Carter, M., Manyin, M., Messen, D., and Burian, S. (2010). The impact of urbanization on current and future coastal precipitation: A case study for Houston. *Environment and Planning B: Planning and Design* **37**(2), 284–304.
- Sismanidis, P., Keramitsoglou, I., and Kiranoudis, C. T. (2015). A satellite-based system for continuous monitoring of Surface Urban Heat Islands. *Urban Climate* **14**(Part 2), 141–153.
- Smith, M., and Emberlin, J. (2006). A 30-day-ahead forecast model for grass pollen in north London, United Kingdom. *International Journal of Biometeorology* **50**(4), 233–242.
- Sobral, H. R. (2005). Heat island in São Paulo, Brazil: Effects on health. *Critical Public Health* **15**(2), 147–156.
- Solecki, W., Rosenzweig, C., Blake, R., de Sherbinin, A., Matte, T., Moshary, F., Rosenzweig, B., Arend, M., Gaffin, S., Bou-Zeif, E., Rule, K., Sweeny, G., and Dessy, W. (2015). New York City Panel on Climate Change 2015 Report: Indicators and monitoring. *Annals of the New York Academy of Science* **1336**, 89–106.
- Stone, B. (2007). Urban and rural temperature trends in proximity to large US cities: 1951–2000. *International Journal of Climatology* **27**(13), 1801–1807.
- Stone, B. (2009). Land use as climate change mitigation. *Environmental Science & Technology* **43**(24), 9052–9056.
- Strauss, B. H., Ziemiński, R., Weiss, J. L., and Overpeck, J. T. (2012). Tidally adjusted estimates of topographic vulnerability to sea level rise and flooding for the contiguous United States. *Environmental Research Letters* **7**(1), 014033.
- Streutker, D. R. (2003). Satellite-measured growth of the urban heat island of Houston, Texas. *Remote Sensing of Environment* **85**(3), 282–289.
- Sweet, W. V., and Park, J. (2014). From the extreme to the mean: Acceleration and tipping points of coastal inundation from sea level rise. *Earth’s Future* **2**(12), 579–600.
- Syvitski, J. P. M., Kettner, A. J., Overeem, I., Hutton, E. W. H., Hannon, M. T., Brakenridge, G. R., Day, J., Vorosmarty, C., Saito, Y., Giosan, L., and Nicholls, R. J. (2009). Sinking deltas due to human activities. *Nature Geoscience* **2**(10), 681–686.
- Takahashi, H., Mikami, T., and Takahashi, H. (2009). Influence of the urban heat island phenomenon in Tokyo in land and sea breezes. In *The Seventh International Conference on Urban Climate*, Yokohama, Japan.
- Tam, B. Y., Gough, W. A., and Mohsin, T. (2015). The impact of urbanization and the urban heat island effect on day-to-day temperature variation. *Urban Climate* **12**(0), 1–10.
- Tan, J., Zheng, Y., Tang, X., Guo, C., Li, L., Song, G., Zhen, X., Yuan, D., Kalkstein, A., Li, F., and Chen, H. (2010). The urban heat island and its impact on heat waves and human health in Shanghai. *International Journal of Biometeorology* **54**(1), 75–84.
- Tayanc, M., and Toros, H. (1997). Urbanization effects on regional climate change in the case of four large cities of Turkey. *Climatic Change* **35**(4), 501–524.
- Taylor, K. E., Stouffer, R. J., and Meehl, G. A. (2012). An overview of CMIP5 and the experiment design. *Bulletin of the American Meteorological Society* **93**(4), 485–498.
- Tran, H., Uchiyama, D., Ochi, S., and Yasuoka, Y. (2006). Assessment with satellite data of the urban heat island effects in Asian mega cities. *International Journal of Applied Earth Observation and Geoinformation* **8**(1), 34–48.
- Tremeac, B., Bousquet, P., de Munck, C., Pigeon, G., Masson, V., Marchadier, C., Merchat, M., Poef, P., and Meunier, F. (2012). Influence of air conditioning management on heat island in Paris air street temperatures. *Applied Energy* **95**(0), 102–110.
- Trenberth, K. E., Jones, P. D., Ambenje, P., Bojariu, R., Easterling, D., Klein Tank, A., Parker, D., Rahimzadeh, F., Renwick, J. A., Rusticucci, M., Soden, B., and Zhai, P. (2007). Observations: Surface and atmospheric climate change. In Solomon, S., Qin, D., Manning, M., Chen, Z., Marquis, M., Averyt, K. B., Tignor, M., and Miller, H. L. (eds.), *Climate Change 2007: The Physical Science Basis. Contribution of Working Group I to the Fourth Assessment Report of the Intergovernmental Panel on Climate Change*. Cambridge University Press.
- Vanhuyse, S., Depireux, J., and Wolff, E. (2006). *Etude de l’évolution de l’impermeabilisation du sol en région de Bruxelles-Capitale*. Université Libre de Bruxelles, IGEAT.
- Vardoulakis, E., Karamanis, D., Fotiadi, A., and Mihalakakou, G. (2013). The urban heat island effect in a small Mediterranean city of high summer temperatures and cooling energy demands. *Solar Energy* **94**, 128–144.
- Vaughan, C. (2016). *An Institutional Analysis of the IPCC Task Group on Data and Scenario Support for Impacts and Climate Analysis (TGI-CA)*. IPCC Task Group on Data and Scenario Support for Impacts and Climate Analysis, Geneva, Switzerland.
- Vietnam Climate Adaptation PartnerShip. (2013). *Ho Chi Minh City Climate Adaptation Strategy*. Vietnam Climate Adaptation Partnership.

- Visbeck, M. H., Hurrell, J. W., Polvani, L., and Cullen, H. M. (2001). The North Atlantic Oscillation: Past, present, and future. *Proceedings of the National Academy of Sciences* **98**(23), 12876–12877.
- Walsh, C. L., Roberts, D., Dawson, R. J., Hall, J. W., Nickson, A., and Hounsome, R. (2013). Experiences of integrated assessment of climate impacts, adaptation and mitigation modelling in London and Durban. *Environment and Urbanization* **25**(2), 361–380.
- Weiss, J. L., Overpeck, J. T., and Strauss, B. (2011). Implications of recent sea level rise science for low-elevation areas in coastal cities of the conterminous USA *Climatic Change* **105**(3), 635–645.
- Willows, R., Reynard, N., Meadowcroft, I., and Connell, R. (2003). *Climate Adaptation: Risk, Uncertainty and Decision-making*. UKCIP Technical Report, UK Climate Impacts Programme.
- Wood, C. R., Järvi, L., Kouznetsov, R. D., Nordbo, A., Joffre, S., Drebs, A., Vihma, T., Hirsikko, A., Suomi, I., Fortelius, C., O'Connor, E., Moiseev, D., Haapanala, S., Moilanen, J., Kangas, M., Karppinen, A., Vesala, T., and Kukkonen, J. (2013). An overview of the urban boundary layer atmosphere network in Helsinki. *Bulletin of the American Meteorological Society* **94**(11), 1675–1690.
- Yang, X., Hou, Y., and Chen, B. (2011). Observed surface warming induced by urbanization in east China. *Journal of Geophysical Research: Atmospheres* **116**(D14).
- Yin, J., Schlesinger, M. E., and Stouffer, R. J. (2009). Model projections of rapid sea-level rise on the northeast coast of the United States. *Nature Geoscience* **2**(4), 262–266.
- Zambrano-Barragán, C., Zevallos, O., Villacis, M., and Enríquez, D. (2011). Quito's climate change strategy: A response to climate change in the metropolitan district of Quito, Ecuador. In Otto-Zimmerman, K. (ed.), *Resilient Cities: Cities and Adaptation to Climate Change Proceedings of the Global Forum 2010* (515–529). Springer Science and Business Media.
- Zauli, S., Scotto, F., Lauriola, P., Galassi, F., and Montanari, A. (2004). Urban air pollution monitoring and correlation properties between fixed-site stations. *Journal of the Air & Waste Management Association* **54**(10), 1236–1241.
- Zhang, C. (2005). Madden-Julian Oscillation. *Reviews of Geophysics* **43**(2).
- Zhang, G. J., Cai, M., and Hu, A. (2013a). Energy consumption and the unexplained winter warming over northern Asia and North America. *Nature Climate Change* **3**(5), 466–470.
- Zhang, H., Qi, Z., -F., Ye, X. -Y., Cai, Y. -B., Ma, W. -C., and Chen, M. -N. (2013b). Analysis of land use/land cover change, population shift, and their effects on spatiotemporal patterns of urban heat islands in metropolitan Shanghai, China. *Applied Geography* **44**, 121–133.
- Zhao, L., Lee, X., Smith, R. B., and Oleson, K. (2014). Strong contributions of local background climate to urban heat islands. *Nature* **511**(7508), 216–219.
- Zhou, Z. -Q., Xie, S. -P., Zheng, X. -T., Liu, Q., and Wang, H. (2014). Global warming-induced changes in El Niño teleconnections over the North Pacific and North America. *Journal of Climate* **27**(24), 9050–9064.
- Hamdi, R., and Schayes, G. (2008). Sensitivity study of the urban heat island intensity to urban characteristics. *International Journal of Climatology* **28**(7), 973–982.
- Hamdi, R., and Van de Vyver, H. (2011). Estimating urban heat island effects on near-surface air temperature records of Uccle (Brussels, Belgium): An observational and modeling study. *Advances in Science and Research* **6**, 27–34.
- Hua, L. J., Ma, Z. G., and Guo, W. D. (2008). The impact of urbanization on air temperature across China. *Theoretical and Applied Climatology* **93**(3–4), 179–194.
- Kalnay, E., and Cai, M. (2003). Impact of urbanization and land-use change on climate. *Nature* **423**(6939), 528–531.
- Landsberg, H. E. (1981). *The Urban Climate*. Academic Press.
- Peel, M. C., Finlayson, B. L., and McMahon, T. A. (2007). Updated world map of the Köppen-Geiger climate classification. *Hydrology and Earth System Sciences Discussions* **4**(2), 462.
- Vanhuyse, S., Depireux, J., and Wolff, E. (2006). *Etude de l'évolution de l'imperméabilisation du sol en région de Bruxelles-Capitale*. Université Libre de Bruxelles, IGEAT.
- World Bank. (2017). 2016 GNI per capita, Atlas method (current US\$). Accessed August 9, 2017: <http://data.worldbank.org/indicator/NY.GNPP.CAP.CD>

Case Study 2.2 Los Angeles Megacities Carbon Project

- Breon, F.M., et al. (2014). An attempt at estimating Paris area CO₂ emissions from atmospheric concentration measurements, *Atmos. Chem. Phys. Discuss.*, **14**, 9647–9703, 2014. Accessed January 21, 2015: www.atmos-chem-phys-discuss.net/14/9647/2014/ doi:10.5194/acpd-14-9647-2014
- Duren, R., and C. E. Miller. (2012). Measuring the carbon emissions of megacities. *Nature Climate Change* **2** (8) 560–562. doi:10.1038/nclimate1629.
- Gurney, K. R., Razlivanov, I., Song, Y. Zhou, Y., Benes, B., and Abdul-Massih, M. (2012). Quantification of fossil fuel CO₂ at the building/street scale for a large US city. *Environmental Science and Technology* **46** (21), 12194–12202. dx.doi.org/10.1021/es3011282.
- Hutyra, L. R., Duren, R., Gurney, K. R., Grimm, N., Kort, E. A., Larson, E., and Shrestha, G. (2014). Urbanization and the carbon cycle: Current capabilities and research outlook from the natural sciences perspective. *Earth's Future* **2**(10), 473–495.
- Kort, E. A., Angevine, W., Duren, R., and Miller, C. E. (2013). Surface observations for monitoring urban fossil fuel CO₂ emissions: minimum site location requirements for the Los Angeles megacity, *Journal of Geophysical Research* **118**, 1577–1584. doi: 10.1002/jgrd.50135.
- Kort, E. A., Frankenberg, C., Miller, C. E., and Oda, T. (2012). Space-based observations of megacity carbon dioxide. *Geophysical Research Letters* **39**, L17806. doi:10.1029/2012GL052738
- Mendoza, D., Gurney, K. R., Geethakumar, S., Chandrasekaran, V., Zhou, Y., and Razlivanov, I. (2013). US regional greenhouse gas emissions mitigation implications based on high-resolution on road CO₂ emissions estimation. *Energy Policy* **55**, 386–395.
- NRC. (2010). *Verifying Greenhouse Gas Emissions: Methods to Support International Climate Agreements*. National Academies Press.
- Peel, M. C., Finlayson, B. L., and McMahon, T. A. (2007). Updated world map of the Köppen-Geiger climate classification. *Hydrology and Earth System Sciences Discussions* **4**(2), 462.
- Silva, S. J., Arellano, A. F., and Worden, H. M. (2013). Toward anthropogenic combustion emission constraints from space-based analysis of urban CO₂/CO sensitivity. *Geophysical Research Letters* **40**(18), 4971–4976.
- U.S. Census Bureau (2010). 2010 Census Data. Accessed December 21, 2014: <http://www.census.gov/topics/population/data.html>
- Wong, K. W., Fu, D., Pongetti, T. J., Newman, S., Kort, E. A., Duren, R., Hsu, Y.-K., Miller, C. E., Yung, Y. L., and Sander, S. P. (2015). Mapping CH₄ : CO₂ ratios in Los Angeles with CLARS-FTS from Mount Wilson, California. *Atmospheric Chemistry and Physics* **15**, 241–252. doi:10.5194/acp-15-241-2015.

Chapter 2 Case Study References

Case Study 2.1 Urban Heat Island in Brussels

- Camuffo, D., and Jones, P. (2002). Improved understanding of past climatic variability from early daily European instrumental sources. In Camuffo, D., and Jones, P. (eds.), *Improved Understanding of Past Climatic Variability from Early Daily European Instrumental Sources* (1–4). Springer Netherlands.
- Demarée, G. R., Lachaert, P. J., Verhoeve, T., and Thoen, E. (2002). The long-term daily Central Belgium Temperature (CBT) series (1767–1998) and early instrumental meteorological observations in Belgium. *Climatic Change* **53**(1–3), 269–293.
- Fricke, R., and Wolff, E. (2002). The MURBANDY Project: Development of land use and network databases for the Brussels area (Belgium) using remote sensing and aerial photography. *International Journal of Applied Earth Observation and Geoinformation* **4**(1), 33–50.

- World Bank. (2010). *Cities and Climate Change: An Urgent Agenda*. World Bank.
- World Bank. (2017). 2016 GNI per capita, Atlas method (current US\$). Accessed August 9, 2017: <http://data.worldbank.org/indicator/NY.GNP.PCAP.CD>
- Wunch, D., Wennberg, P. O., Toon, G. C., Keppel-Aleks, G., and Yavin, Y. G. (2009). Emissions of greenhouse gases from a North American megacity. *Geophysical Research Letters* **36**, L15810. doi:10.1029/2009GL039825.
- Case Study 2.3 Rio de Janeiro Impacts of the Madden-Julian Oscillation**
- Corpo de Bombeiros. (2014). *Histórico do Corpo de Bombeiros Militar do Estado do Rio de Janeiro*. Accessed September 7, 2015: <http://www.cbmerj.rj.gov.br>.
- Costa, H., and Teuber, W. (2001). *Enchentes no Estado do Rio de Janeiro: Uma abordagem geral*. SEMADS.
- Dereczynski, C. P., Oliveria, J. S., and Machado, C. O. (2009). Climatologia da precipitação no município do Rio de Janeiro. *Revista Brasileira de Meteorologia* **24**(1), 24–38.
- Grimm, A. M., and Tedeschi, R. G. (2009). ENSO and extreme rainfall events in South America. *Journal of Climate* **22**(7), 1589–1609.
- Peel, M. C., Finlayson, B. L., and McMahon, T. A. (2007). Updated world map of the Köppen-Geiger climate classification. *Hydrology and Earth System Sciences Discussions* **4**(2), 462.
- Tedeschi, R. G., Grimm, A. M., and Cavalcanti, I. F. A. (2015). Influence of Central and East ENSO on extreme events of precipitation in South America during austral spring and summer. *International Journal of Climatology* **35**(8), 2045–2064.
- Universidade Estadual de Londrina (UEL). (2014). Cidade alagada: Chuvas de verão, classe e estado no Rio de Janeiro 1966–1967.
- United Nations Disaster Relief Organization (UNDRO). (1988). Brazil – Floods Feb 1988 UNDRO Information Reports 1–5.
- World Bank. (2017). 2016 GNI per capita, Atlas method (current US\$). Accessed August 9, 2017: <http://data.worldbank.org/indicator/NY.GNP.PCAP.CD>
- Case Study 2.4 Will Climate Change Induce Malaria in Nairobi?**
- Cox, J., Craig, M., Le Sueur, D., and Sharp, B. (1999). *Mapping Malaria Risk in the Highlands of Africa*. MARA/HIMAL Technical Report (96).
- Ermert, V., Fink, A. H., Morse, A. P., and Paeth, H. (2012). The impact of regional climate change on malaria risk due to greenhouse forcing and land-use changes in tropical Africa. *Environmental Health Perspectives* **120**(1), 77.
- Hay, S. I., Cox, J., Rogers, D. J., Randolph, S. E., Stern, D. I., Shanks, G. D., Myers, M. F., and Snow, R. W. (2002). Climate change and the resurgence of malaria in the East African highlands. *Nature* **415**(6874), 905–909.
- Hashizume, M., Chaves, L. F., and Minakawa, N. (2012). Indian Ocean Dipole drives malaria resurgence in East African highlands. *Scientific Reports* **2**, 269.
- IPCC. (2013). *Climate Change 2013: The Physical Science Basis. Contribution of Working Group I to the Fifth Assessment Report of the Intergovernmental Panel on Climate Change*. Cambridge University Press.
- Kim, Y.-M., Park, J.-W., and Cheong, H.-K. (2012). Estimated effect of climatic variables on the transmission of Plasmodium vivax malaria in the Republic of Korea. *Environmental Health Perspectives* **120**(9), 1314.
- Peel, M. C., Finlayson, B. L., and McMahon, T. A. (2007). Updated world map of the Köppen-Geiger climate classification. *Hydrology and Earth System Sciences Discussions* **4**(2), 462.
- Shanks, G. D., Hay, S. I., Omumbo, J. A., and Snow, R. W. (2005). Malaria in Kenya's western highlands. *Emerging Infectious Diseases* **11**(9), 1425–1432.
- Smith, K. R., Woodward, A., Campbell-Lendrum, D., Chadee, D. D., Honda, Y., Liu, Q., Olwoch, J. M., Revich, B., and Sauerborn, R. (2014). Human health: Impacts, adaptation, and co-benefits. In Field, C. B., Barros, V. R., Dokken, D. J., Mach, K. J., Mastrandrea, M. D., Bilir, T. E., Chatterjee, M., Ebi, K. L., Estrada, Y. O., Genova, R. C., Girma, B., Kissel, E. S., Levy, A. N., MacCracken, S., Mastrandrea, P. R., and White, L. L. (eds.), *Climate Change 2014: Impacts, Adaptation, and Vulnerability. Part A: Global and Sectoral Aspects. Contribution of Working Group II to the Fifth Assessment Report of the Intergovernmental Panel of Climate Change* (709–754). Cambridge University Press.
- Tonui, W. K. S., Otor, C. J., Kabiru, E. W., and Kiplagat, W. K. (2013). Patterns and trends of malaria morbidity in western highlands of Kenya. *International Journal of Education and Research* **1**(12), 1–8.
- World Bank. (2017). 2016 GNI per capita, Atlas method (current US\$). Accessed August 9, 2017: <http://data.worldbank.org/indicator/NY.GNP.PCAP.CD>
- Case Study 2.5 Climate Extreme Trends in Seoul**
- Chi, Y., Zhang, F., Li, W., He, J., and Guan, Z. (2014). Correlation between the onset of the east Asian subtropical summer monsoon and the eastward propagation of the Madden-Julian Oscillation. *Journal of the Atmospheric Sciences* **72**(3), 1200–1214.
- Demographia (2016). *Demographia World Urban Areas 2016*. Accessed August 9, 2017: <http://www.demographia.com/db-worldua.pdf>
- Lee, S. H., and Baik, J.-J. (2010). Statistical and dynamical characteristics of the urban heat island intensity in Seoul. *Theoretical and Applied Climatology* doi: 10.1007/s00704-009-0247-1.
- Peel, M. C., Finlayson, B. L., and McMahon, T. A. (2007). Updated world map of the Köppen-Geiger climate classification. *Hydrology and Earth System Sciences Discussions* **4**(2), 462.
- Son, J.-Y., Lee, J.-T., Anderson, B., and Bell, M. L. (2012). The impact of heat waves on mortality in seven major cities in Korea. *Environmental Health Perspectives* **120**(4), 566–571.
- World Bank. (2017). 2016 GNI per capita, Atlas method (current US\$). Accessed August 9, 2017: <http://data.worldbank.org/indicator/NY.GNP.PCAP.CD>